Structural and seismological segmentation of the Gulf of Corinth fault system: implications for models of fault growth

Gerald P. Roberts[1](*) **and Ioannis Koukouvelas**[2]

[1] *Research School of Geological and Geophysical Sciences, Birkbeck College and University College London, U.K.*

[2] *Department of Geology, University of Patras, Greece*

Abstract

The positions and dimensions of fault segments within the Gulf of Corinth fault system have been identified by analysing spatial variation in fault displacements and fault kinematics. Growth of these fault segments is assessed by comparing their geometry and kinematics with the geometry and kinematics of the three sets of earthquake surface ruptures that are known to have affected the area in the last ~200 years. Areas along the Gulf of Corinth fault system exhibiting low fault displacement (tens of metres) are identified as persistent segment boundaries which separate the fault system into a number of fault segments characterised by displacements which achieve maxima of ~3 km. Fault-slip directions defined by lineations on fault planes vary systematically with fault displacement, showing a converging pattern towards the hanging-walls of the fault segments: the fault-slip directions change by ~90° across persistent segment boundaries. It is unclear where fault segments end and persistent segment boundaries begin, but if the persistent segment boundaries are considered to be ~10-15 km across, the intervening fault segments achieve lengths of 30-35 km. In contrast known surface ruptures during the last ~200 years, including those for the 1995 Egion earthquakes, have all been < 15 km in length: these so-called *earthquake segments* are, therefore, considerably shorter than the *fault segments* that hosted the earthquakes. Also, the positions of *earthquake segments* have varied relative to the positions of the *fault segments* during successive earthquakes. It appears, therefore, that a Modified Overlap Model is more appropriate than the Characteristic Earthquake Model to describe the seismological behaviour of fault segments around the Gulf of Corinth through a number of earthquake cycles. A pattern of coseismic slip vectors converging towards the hanging-wall has been measured for the surface ruptures to 1995 Egion earthquakes; a similar pattern was noted for the 1981 Alkyonides earthquake ruptures. Repetition of such ruptures in different positions along fault segments, in accordance with a Modified Overlap Model, will produce systematic variations in the scatter of fault-slip directions with fault displacement. Thus, scatter in the orientations of lineations on fault planes may contain information concerning the lengths and positions of numerous pre-historic earthquake segments; information which may be used to constrain both the palaeoseismology and the future seismicity in areas of active extension.

Key words *segmentation – fault-slip data – surface ruptures – characteristic earthquakes*

1. Introduction

It is well known that although normal fault systems can continue for hundreds of kilometres along strike, only short segments measur-

ing a few tens of kilometres in length are ruptured during normal faulting earthquakes (Jackson and White, 1989; Crone and Haller, 1991): the portions of the fault system ruptured during a single earthquake are known as *earthquake segments* (*sensu* Machette *et al.*, 1991; de Polo *et al.*, 1991). Because the area of the ruptured fault surface, defined by the length of a surface rupture and the down-dip width of the fault, shows a direct relationship with the

(*) e-mail: gerald.roberts @ ucl.ac.uk

magnitude of the causative earthquake (Wyss, 1979; Hanks and Kanamori, 1979; Bonilla *et al.*, 1984; Abercrombie and Leary, 1993), the recognition of the dimensions of rupture-prone segments of fault systems forms the basis for prediction of maximum earthquake magnitudes in a region, and hence seismic hazard assessment.

Predicting the lengths of future rupture-prone segments along active normal faults is accomplished most reliably using palaeoseismological observations of the dimensions of ancient surface ruptures as a guide. For example, in the Basin and Range province, Western U.S.A., numerous pre-historic and historical ruptures have formed scarps a few metres high whose lengths have been mapped providing a basis for predicting the lengths of future earthquake ruptures (de Polo *et al.*, 1991; Machette *et al.*, 1991; Crone and Haller, 1991).

However, in Central Greece this methodology cannot be used at present because a comparatively-poor palaeoseismological record exists for the area. A comprehensive record of all the large magnitude earthquakes that have occurred in the last ~100 years is available, but only three events are known to have produced significant surface faulting onshore in the last ~200 years; the 1995 Egion earthquakes, the 1981 Alkyonides earthquakes and the 1861 Egion earthquakes (Jackson *et al.*, 1982; Ambraseys and Jackson, 1990; Mouyaris *et al.*, 1992). Information concerning historical earthquakes prior to ~200 years ago is probably incomplete because historical accounts are lacking for some remote regions (Ambraseys and Jackson, 1990; Mouyaris *et al.*, 1992; Koukouvelas and Doutsos, submitted); there are no accounts of surface faulting during earthquakes. The nature of pre-historic earthquakes is largely un-known: the best information comes from records of uplifted coastal notches, but these records are at best region-specific and cannot differentiate between earthquakes hosted by different faults (Stewart, 1996). Thus, because the palaeoseismological record is incomplete for periods of time covering > ~200 years, and only contains information concerning three surface ruptures, it may be premature to use this record to predict future fault behaviour. It may be that larger or, conversely, smaller ruptures are more common when viewed over longer time periods. Also, fault slip rates, earthquake frequency and/or magnitudes may also vary over periods of time > 200 years with a consequent temporal variation in seismic hazards (*e.g.*, Machette *et al.*, 1991; Mouyaris *et al.*, 1992): information concerning numerous palaeo-earthquakes is needed before these uncertainties are removed.

This paper attempts to assess the likely nature of numerous palaeo-earthquakes around the Gulf of Corinth by: 1) identifying persistent segment boundaries, that is, areas of low fault displacement where numerous earthquake ruptures have terminated or been interrupted in the past (Wheeler, 1989; Machette *et al.*, 1991; Zhang *et al.*, 1991); 2) assessing the growth of the fault segments lying between these persistent segment boundaries by examining the geometry and kinematics of the three surface faulting events that have occurred in the last ~200 years. *Fault segments* are defined herein as areas of the fault system with relatively large fault displacement (several kilometres) that lie between persistent segment boundaries marked by low fault displacements (tens of metres). Small-scale geometric offsets between faults are not used to define fault segment boundaries in this study and the reasons for this are discussed by Roberts (1996). The aim of this methodology is to assess whether the Characteristic Earthquake Model or one of a number of alternative models (Schwartz, 1989; Scholz, 1989) (fig. 1) is most appropriate to describe the long-term seismological behaviour of the Gulf of Corinth fault system. Long-term is considered in this study to be a period of time long enough to include numerous earthquake cycles associated with large (> M_s 6.0) magnitude earthquakes on a single fault segment. Note that the Characteristic Earthquake Model (fig. 1) implies that the along-strike length of *fault segments* should be the same as that of *earthquake segments*: thus, it should be possible to use the length of the fault segments to constrain the likely lengths of future ruptures. Also, because earthquake recurrence in the Characteristic Earthquake Model is time- and slip-predictable, and consistent along the length of a fault segment, palaeoseismological

observations at one locality along a fault segment can be used to predict past and future patterns of fault activity at other locations along the same fault segment. However, note that alternative models of long-term seismological behaviour show no such relationships (fig. 1) so that it is clearly important to utilise the correct behaviour model when assessing seismic hazards using a probabilistic approach.

Firstly, a brief summary of the geological and seismological nature of the area around the Gulf of Corinth is given, followed by descriptions of the ten fault segments identified in this study area. Secondly, reviews of the geometry and kinematics of the surface ruptures to the 1861 Egion earthquakes and the 1981 Alkyonides earthquakes are given together with new descriptions for the 1995 Egion earthquakes. Finally, models of fault growth are discussed before some conclusions concerning the long-term seismological behaviour of the Gulf of Corinth fault system are presented.
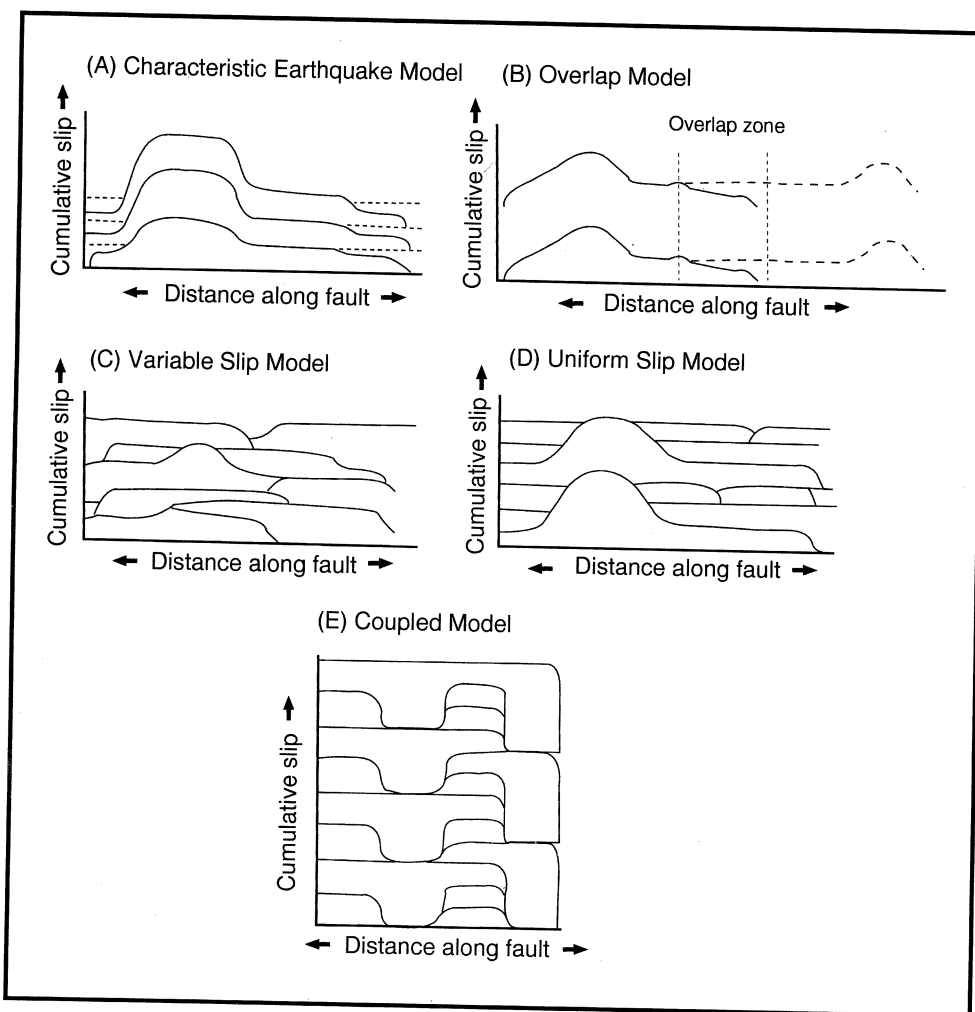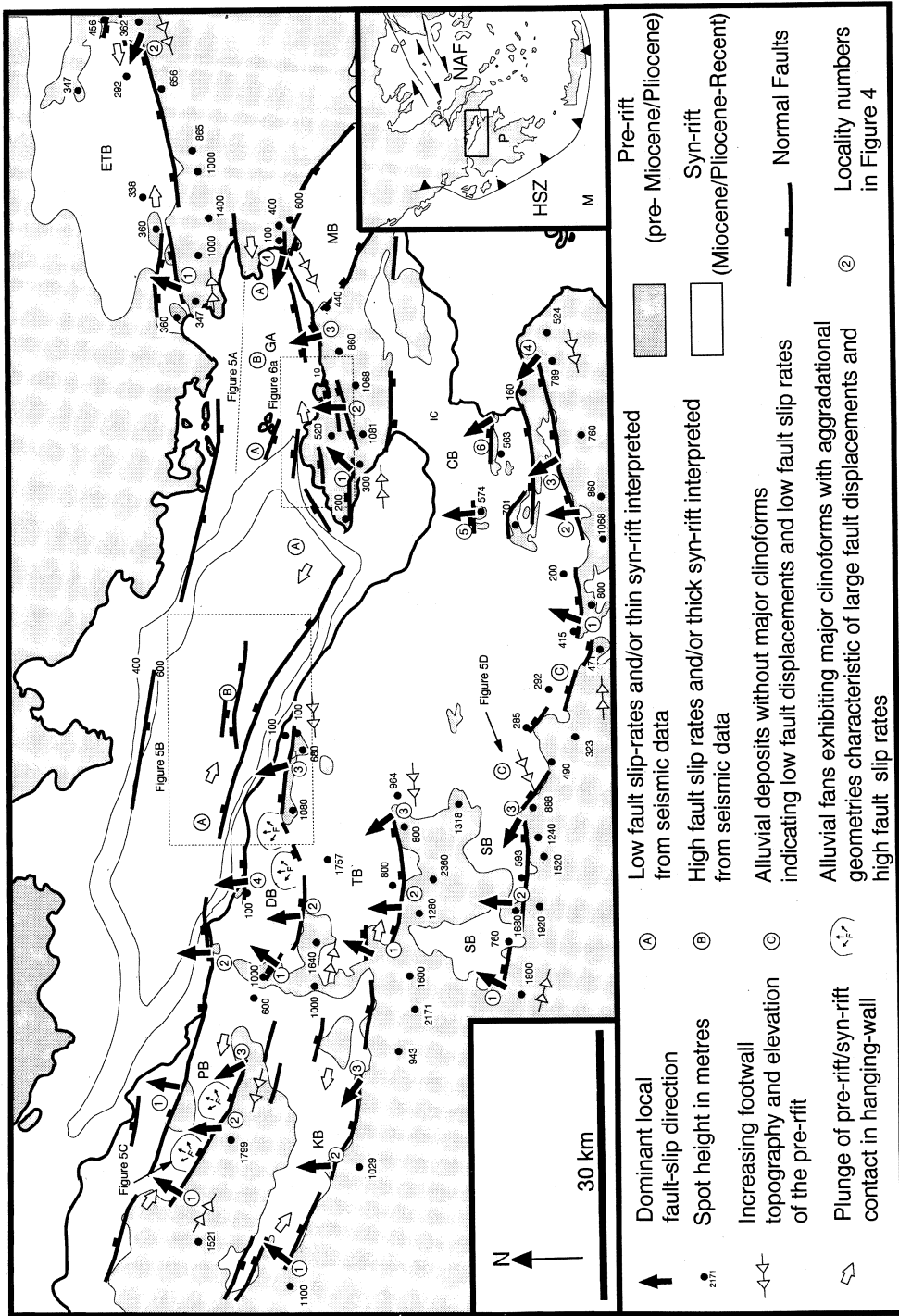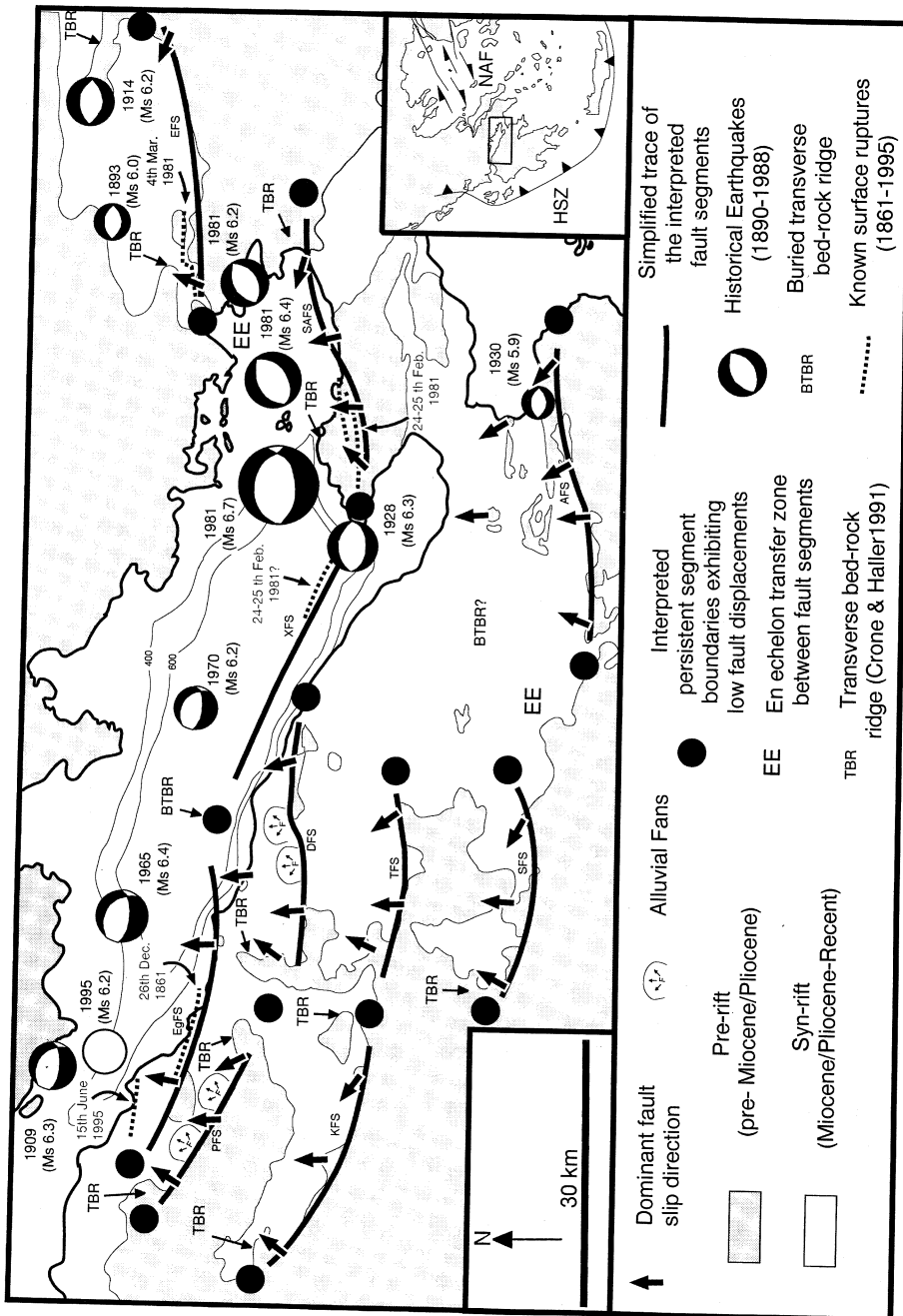

Fig. 1. Models of fault behaviour (adapted from Schwartz, 1989 and Scholz, 1989).

Fig. 2a. Map showing the geology, topography and bathymetry of the area around the Gulf of Corinth.

Fig. 2b. Interpretation of fig. 2a showing the positions of fault segments, persistent segment boundaries and historical earthquakes around the Gulf of Corinth. CB = Corinth Basin; GA = Gulf of Alkyonides; MB = Megara Basin; ETB = Erithres/Thiva Basin; DB = Derveni Basin; PB = Pteri Basin; KB = Kalavrita Basin; TB = Trikala Basin; SB = Stimfalia Basin; M = Mediterranean; P = Peloponnese; IC = Isthmus of Corinth; HSZ = Hellenic Subduction Zone; NAF = North Anatolian Fault; KFS = Kalavrita Fault Segment; PFS = Pteri Fault Segment; EgFS = Egion Fault Segment; DFS = Derveni Fault Segment; TFS = Trikala Fault Segment; SFS = Stimfalia Fault Segment; XFS = Xilokastro Fault Segment; AFS = Athikia Fault Segment; SAFS = South Alkyonides Fault Segment; EFS = Erithres Fault Segment.

2. Geological and seismological background

The Gulf of Corinth is a 30 km wide inlet of the Mediterranean stretching 120 km along a WNW-ESE trend (fig. 2a). The Peloponnese Peninsula lies to the south of the Gulf of Corinth, separated from the rest of mainland Greece by the Isthmus of Corinth. The area considered is marked by active ~N-S directed extensional tectonics accommodated by WNW-ESE and ENE-WSW striking normal faults. The area of extension lies to the north of the north-dipping Hellenic subduction zone (Kelletat et al., 1976; Le Pichon and Angelier, 1979; Le Pichon, 1982) and to the west of the major strike-slip systems of the North and East Anatolian Faults (Jackson, 1994). A combination of studies of earthquake focal mechanisms, limited studies of lineations on faults and palaeomagnetic rotations indicate that the active normal faults accommodate north-south extension ($\pm 20°$) within an area of that is undergoing clockwise rotations about vertical axes (Jackson et al., 1982; Vita-Finzi and King, 1985; Roberts and Jackson, 1991; Taymaz et al., 1991; Jackson, 1994 and references therein).

In general, the normal faults with the largest throws dip to the north, and in places there is over 3000 m of relief between the deepest parts of the Gulf of Corinth, where Neogene syn-rift deposits exist in the hanging-wall, and the peaks of the flanking mountains in the footwall which are composed predominantly of Mesozoic carbonates and silici-clastic rocks (Brooks and Ferentinos, 1984). Seismic reflection data show that the basin in the hanging-wall of the Gulf of Corinth fault system is generally asymmetric, having the geometry of half-graben, containing at least 700 m of syn-rift strata that thin to the north (Myrianthis, 1982; Brooks and Ferentinos, 1984; Higgs, 1988). However, some faults downthrow to the south, south-west or north-east, in particular controlling the positions of the Plio-Pleistocene Corinth and Megara Basins, but no recent seismic activity has been reported along these particular faults.

The Gulf of Corinth has hosted 11 earthquakes of magnitude $> M_s$ 5.8 in the last ~100 years (fig. 2b), but only three earthquake sequences are known to have produced extensive surface breaks on land (Ambraseys and Jackson, 1990, see below). Correlation of the surface ruptures along the faults bounding the southern shores of the Gulf of Alkyonides with the hypocentral locations for the earthquakes of 24-25th February 1981, indicates that the faults are planar down to depths of ~10-14 km and dip at around 40-60° (Jackson et al., 1982; Jackson and White, 1989; Taymaz et al., 1991). Following re-occupation of a number of sites whose relative positions were surveyed in the last century, recent geodetic observations have shown that ~1 m of ~N-S extension has occurred across Central Greece in the last century (Billiris et al., 1991).

3. Methodology for identifying persistent segment boundaries and the intervening fault segments

Following the lead of workers studying fault segmentation in the Basin and Range province of Western U.S.A. (de Polo et al., 1991; Machette et al., 1991; Crone and Haller, 1991), an attempt has been made to identify structural features along the Gulf of Corinth fault system that appear to have behaved as barriers to the lateral propagation of ruptures during a large number of earthquakes cycles. These so-called persistent segment boundaries were identified by examining the magnitude of fault displacements implied by structural geometries on published geological maps and geophysical interpretations. In general the transition from high (several kilometres) to low (tens of metres) fault displacements is revealed by the presence of the following features (see fig. 3).

1) *The lateral termination of hanging-wall basins along the faults* – Because hanging-wall basins are generally the shape of a half-spoons (Roberts and Gawthorpe, 1995) the contact between syn-rift rocks (Miocene/Pliocene and younger in Central Greece) and pre-rift rocks (pre-Miocene) dips basinwards close to persistent segment boundaries. Syn-rift sediments generally thin towards, and onlap onto areas
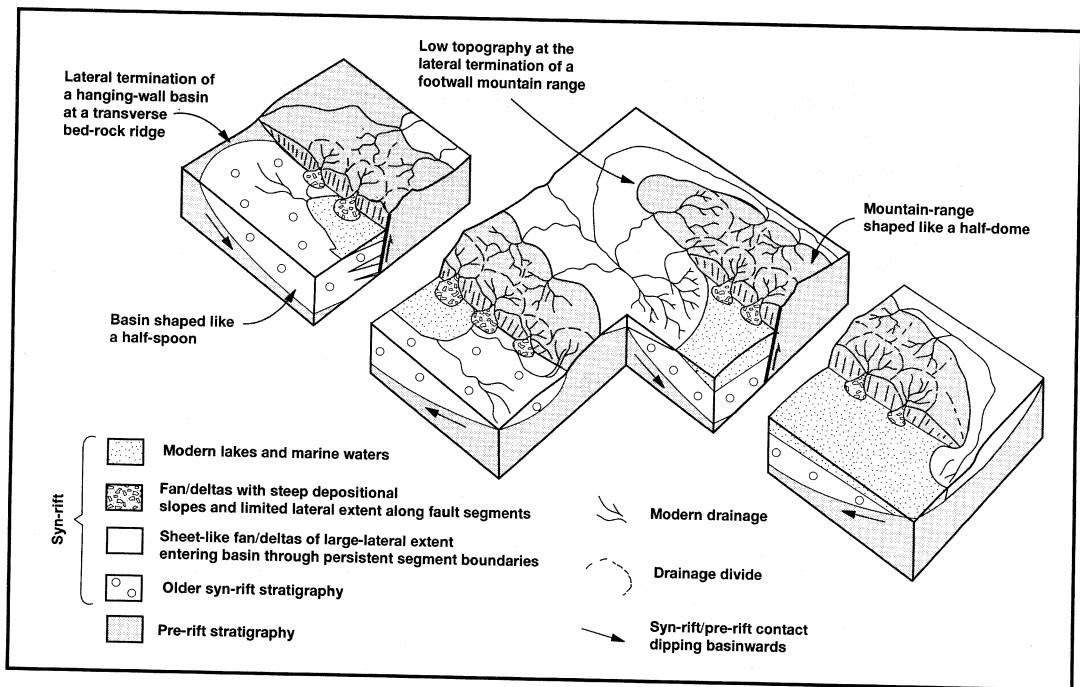
Fig. 3. Block diagram showing the features of segmented normal faults around the Gulf of Corinth (adapted from Roberts and Gawthorpe, 1995).

which mark persistent segment boundaries, whilst palaeocurrents in syn-rift sediments are directed away from them.

2) *The lateral termination of footwall mountain ranges* – Because footwall mountain ranges are the shape of half-domes, areas of low topography mark the positions of persistent segment boundaries. In Central Greece, a large proportion of syn-rift sediments sourced in the footwall mountains enter the hanging-wall basins through such persistent segment boundaries. Fluvial/deltaic depositional systems have a sheet-like geometry, covering large areas (tens of kilometres) and do not show dramatic changes in thickness associated with faults. In contrast, in the centre of fault segments, sediments sourced in the footwall mountains enter the hanging-wall through incised gorges feeding depositional systems with high depositional slopes (alluvial fans/fan deltas): sediment thicknesses increase abruptly across the

faults bounding the footwall mountains (Dart *et al.*, 1994; Gawthorpe *et al.*, 1994).

3) *Lateral variations in both the rates and magnitudes of vertical motions* – Both low subsidence rates (revealed by decreasing hanging-wall sediment thicknesses along strike), and low uplift rates (revealed by decreasing elevations along strike of uplifted areas) can be used to define the positions of persistent segment boundaries around the Gulf of Corinth.

At an early stage in the study, it was realised that fault-slip directions vary systematically with fault displacements in the area studied (following field studies by GPR; see Roberts, 1996). As a result, the orientations of 1201 frictional-wear striae and metre-scale corrugations of fault surfaces (*sensu* Hancock and Barka, 1987) were measured by GPR close to the centres of fault segments and bordering persistent segment boundaries (fig. 4): these data can also be used to define the positions of
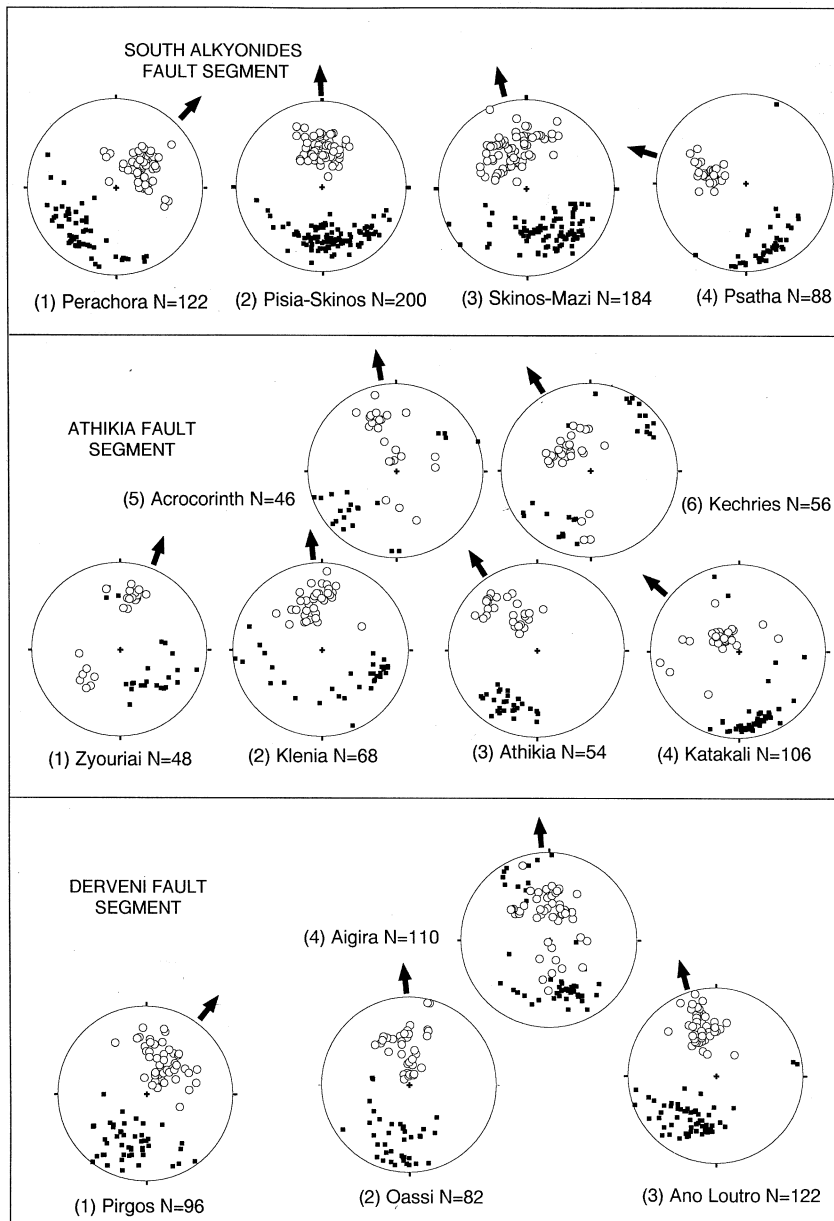
Fig. 4. Lower hemisphere stereographic projections of poles to fault planes (filled squares) and lineations on fault planes (open circles) for the Gulf of Corinth. The 30 localities are named after the closest town or village and the locality numbers are also shown on fig. 2a. Measurements were made (by GPR) of all faults and lineations that intersected traverse lines across exposures. The majority of measurements were taken from the faulted contacts between the pre-rift and syn-rift rocks for the South Alkyonides and Kalavrita Fault Segments, and from the faulted contacts between the pre-rift and syn-rift rocks and fault

626
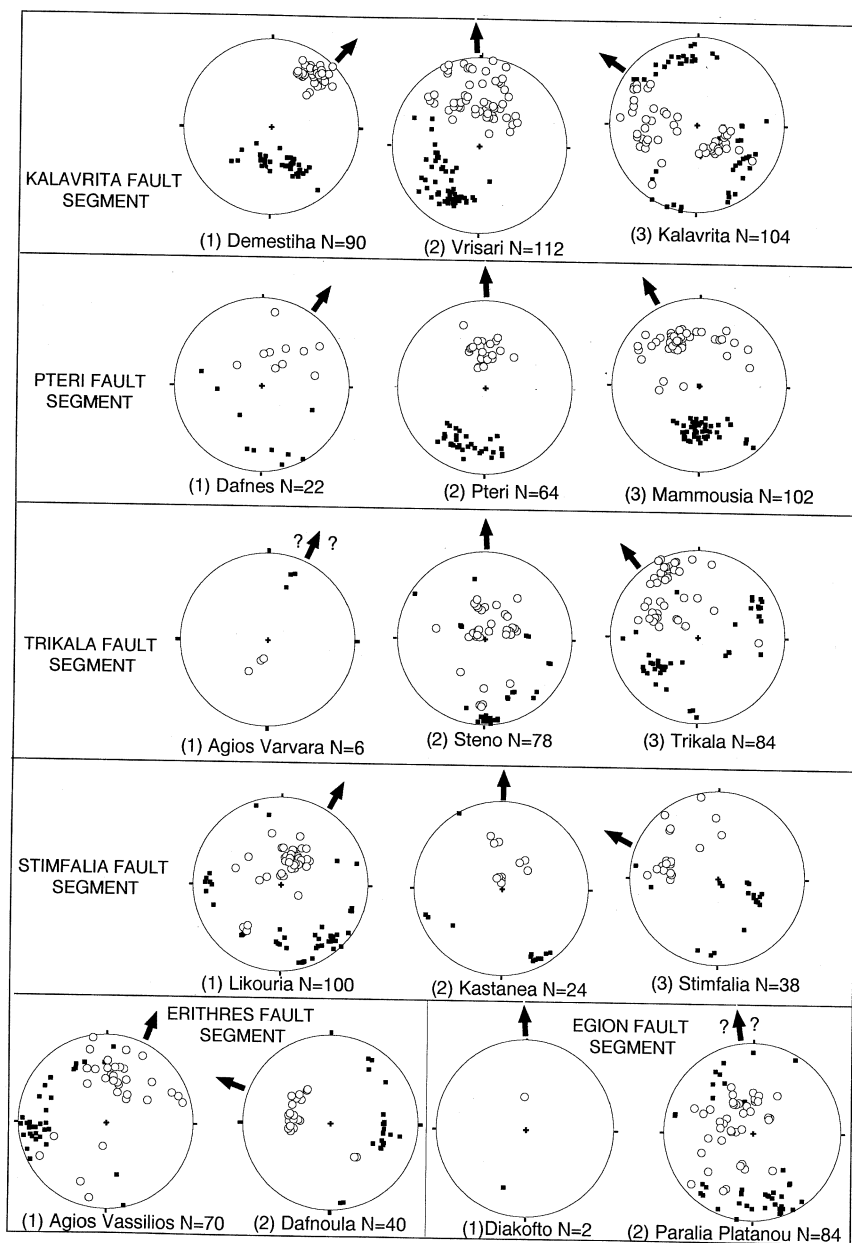
planes located in the footwall of these contacts for the other segments. In the case of the South Alky-onides Fault Segment, measurements for locality 2 were taken from 15 exposures < 400 m^2 in area within an area of ~60 km^2 and from 5 exposures < 400 m^2 in area within an area of ~20 km^2 for locality 4. In all other examples the measurements were taken from single exposures < 400 m^2 in area. Arrows appended to the stereonets give a visual guide to the fault-slip direction interpreted from the stereonet, and these arrows have been transferred onto figs. 2a,b.

627

persistent segment boundaries (see below). All measurements of lineations were taken from fault planes in Mesozoic rocks. These faults either form the main faulted contacts between the syn-rift rocks and pre-rift rocks or are small faults situated within the footwalls, but within ~10 m of the main basin-bounding faults.

4. Fault segments and persistent segment boundaries around the Gulf of Corinth

In this section, persistent segment boundaries around the Gulf of Corinth are identified using the criteria stated in the previous section and the fault segments bounded by persistent segment boundaries are described in turn. Note that fig. 3 shows a rather simplified view of the geometry of fault segments: segments are in fact comprised of a number of smaller faults. In order to illustrate how the fault segments described below are defined, fig. 2a shows the major faults, whilst fig. 2b shows an interpretation where the faults are grouped into fault segments whose simplified map trace is shown (for comparison with fig. 3). As will be shown below, the faults are grouped into segments where it can be demonstrated that they share a coherent pattern of kinematics described by fault-slip directions (see Roberts, 1996, for a description of this methodology). The descriptions of the fault segments presented below are, in places, repetitive, but this is necessary as this is the first time these fault segments have been described.

4.1. *South Alkyonides Fault Segment (SAFS)*

The SAFS is described first as it has been studied in greater detail than the other fault segments (Roberts and Gawthorpe, 1995; Roberts, 1996). A major normal fault system bounds the southern shores of the Gulf of Alkyonides Basin which is the eastern extremity of the Gulf of Corinth (IGME 1984a,c; Perissoratis *et al.*, 1986; Papatheodorou and Ferentinos, 1993). Water depths in the Gulf of

Alkyonides are relatively shallow (< 400 m) compared with water depths further west within the Gulf of Corinth. The basin-bounding fault system hosted surface ruptures to the 1981 Gulf of Corinth earthquakes (M_s 6.7-6.4) (Jackson *et al.*, 1982) (fig. 2b) and may also have been ruptured by a large magnitude event in A.D. 1887 although no surface faulting has been reported for this event (Ambraseys and Jackson, 1990).

Displacement gradients along this fault system can be identified following examination of the spatial variation of the elevation of the top of the Mesozoic rocks shown on published geological maps, seismic reflection profiles and Bougeur gravity maps (IGME, 1984a,c; Myrianthis, 1982) (figs. 5a and 6a-c). Fault displacements vary from a few tens of metres in the areas west of Perachora and east of Psatha to ~3 km offshore of the area between Skinos and Alepochori: hanging-wall subsidence is ~2 km in this area whilst footwall uplift is ~1 km.

In summary, the Alkyonides Basin is shaped like a half-spoon. The bounding faults disappear into areas of low-displacement which are interpreted here to be persistent segment boundaries. These areas have pre-rift rocks exposed at the surface which form transverse ridges extending into the hanging-wall (fig. 2b) which are onlapped by syn-rift sediments (fig. 5a).

Where fault displacements decrease at the western end of the fault segment near the village of Perachora, the dominant fault-slip direction is ~NE-SW (figs. 4 and 6a-c). In contrast, where fault displacements decrease at the eastern end of the fault segment near the village of Psatha the dominant fault-slip direction is ~NW-SE. Finally, in the centre of the fault segment where displacements are greatest between the villages of Pisia and Alepochori the dominant fault-slip direction is ~N-S.

4.2. *Erithres Fault Segment (EFS)*

A major normal fault system bounds the southern margin of the Erithres/Thiva Basin (IGME, 1971, 1984b), which lies close to, but
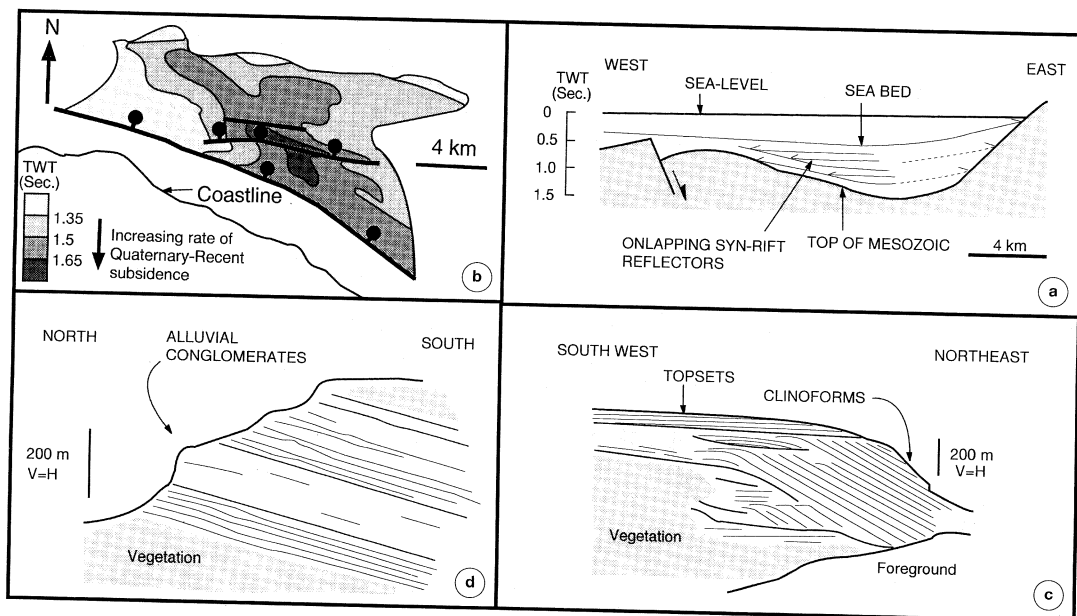
Fig. 5a-d. Variation in the thicknesses and internal geometries of syn-rift deposits around the Gulf of Corinth (see fig. 2a for locations of figures). a) Line drawing of a seismic reflection profile from the Gulf of Alkyonides (adapted from Myrianthis, 1982) with additional information added to the eastern end of the cross-section taken from field observations (GPR) and outcrop data (IGME, 1984a). Prominent syn-rift reflectors (? Pliocene-Recent) onlap Mesozoic basement in the west of the cross-section (Myrianthis, 1982) and Pliocene-recent deposits onlap Mesozoic limestones at the eastern end of the cross-section. The rates and magnitudes of subsidence, and presumably the slip rates on the basin-bounding fault system to the south (SAFS), increase from minima in the east and west to a maxima in the centre of the cross-section. b) Isochron map of the area offshore of Xilokastron, for the interval between a Quaternary syn-rift reflector and the sea-bed (redrawn from Higgs, 1988). The increase in two-way travel-time signifies an increase in sediment thickness. The variations in sediment thickness result from variations in subsidence, and presumably fault-slip rates, from minima in the WNW and ESE to a maxima between these two areas. c) Line drawing of incised gorge sections through the Keranitis Fan/Delta which lies in the hanging-wall of the Pteri Fault Segment (adapted from Gawthorpe et al., 1984, and from field observations by GPR). The large clinoforms and aggradational to progradational sequence geometries result from the palaeo-structural relief and high slip-rates relative to infilling by sediment reported for this location (Dart et al., 1994; Gawthorpe et al., 1994). d) Line drawing of incised gorge sections located at the eastern end of the Stimfalia Fault Segment, through alluvial conglomerates (observations by GPR). The lack of large clinoforms and aggradational to progradational sequence geometries result from the low palaeo-structural relief and low fault-slip rates which characterise this locality.

above sea-level (200-400 m), probably because it is bounded by one of the distal segments of the Gulf of Corinth fault system. The EFS was probably ruptured by earthquakes in 1914 (M_s 6.2) and 1893 (M_s 6.0) (Ambraseys and Jackson, 1990; Mouyaris et al., 1992) although no surface faulting has been reported. Also, antithetic surface faulting associated with the

March 4th, 1981 earthquake (M_s 6.4) occurred within the basin (Jackson et al., 1982).

Displacement gradients along this fault system can be identified following examination of the spatial variation in footwall topography and the dip of the syn-rift to pre-rift contact in the hanging-wall (IGME, 1971, 1984b). The footwall topography increases from minima in the
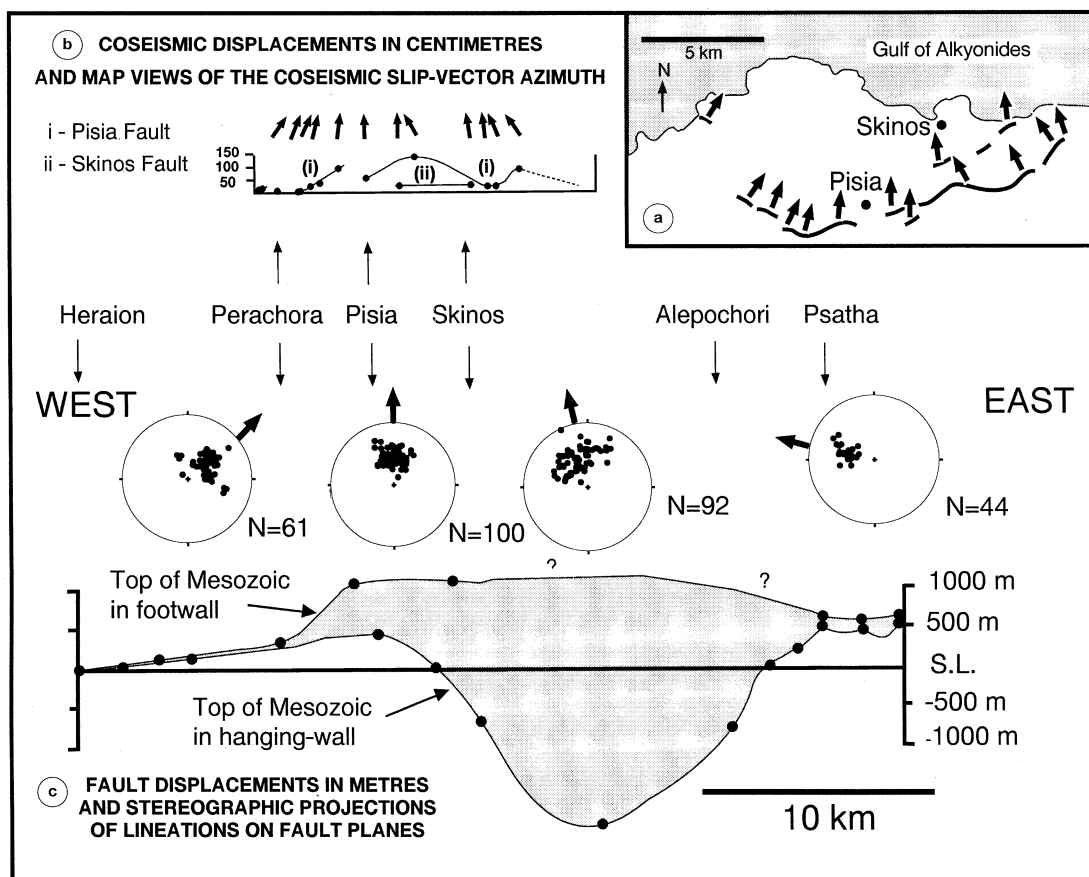
Fig. 6a-c. Comparison of displacements and fault-slip directions associated with the South Alkyonides Fault Segment (SAFS) with scarp heights and co-seismic slip directions for the 24-25th March, 1981 Alkyonides earthquakes. The line of section for fig. 6c runs along the simplified fault segment trace shown for the SAFS in fig. 2b. Note: 1) the existence of lineations on the SAFS plunging towards the ~NE in the Skinos-Ale-pochori area where coseismic slip vectors plunge ~NW, and 2) where the displacements on the SAFS reach a maxima to the east of Skinos, the 1981 scarps die out: these features cannot have been produced by palaeo-ruptures with the same kinematics, displacements and location as those produced during the 1981 earthquakes. The inset map shows a map view of the onshore surface ruptures and associated coseismic slip-vectors for the 24-25th March, 1981 Alkyonides earthquakes.

east and west of the fault segment (< 400 m) to maxima in the centre (~1400 m) (fig. 7) whilst the contact between the pre-rift and syn-rift rocks plunges basinwards in the hanging-wall of the segment (fig. 2a). In summary, like the Alkyonides Basin, the Erithres/Thiva Basin is shaped like a half-spoon whilst the footwall mountain range is shaped like a half-dome.

The basin-bounding faults disappear into areas of low-displacement which are interpreted here as persistent segment boundaries. Transverse bed-rock ridges extend into the hanging-wall from these persistent segment boundaries (fig. 2b).

Where fault displacements decrease at the western end of the fault segment near the vil-

lage of Agios Vasilios, the dominant fault-slip direction is ~NE-SW (figs. 2a,b, 4 and 7). Where fault displacements decrease at the eastern end of the fault segment near the village of Dafnoula, the dominant fault-slip direction is ~NW-SE. No exposures of faults with lineations were found along the centre of the fault segment.

4.3. *Xilokastron Fault Segment (XFS)*

A major normal fault system forms a marked bathymetric escarpment on the floor of the Gulf of Corinth in this region (Brooks and Ferentinos, 1984; Higgs, 1988); water depths to the north of the submarine escarpment are > 600 m. Because the fault is offshore, it is dif-
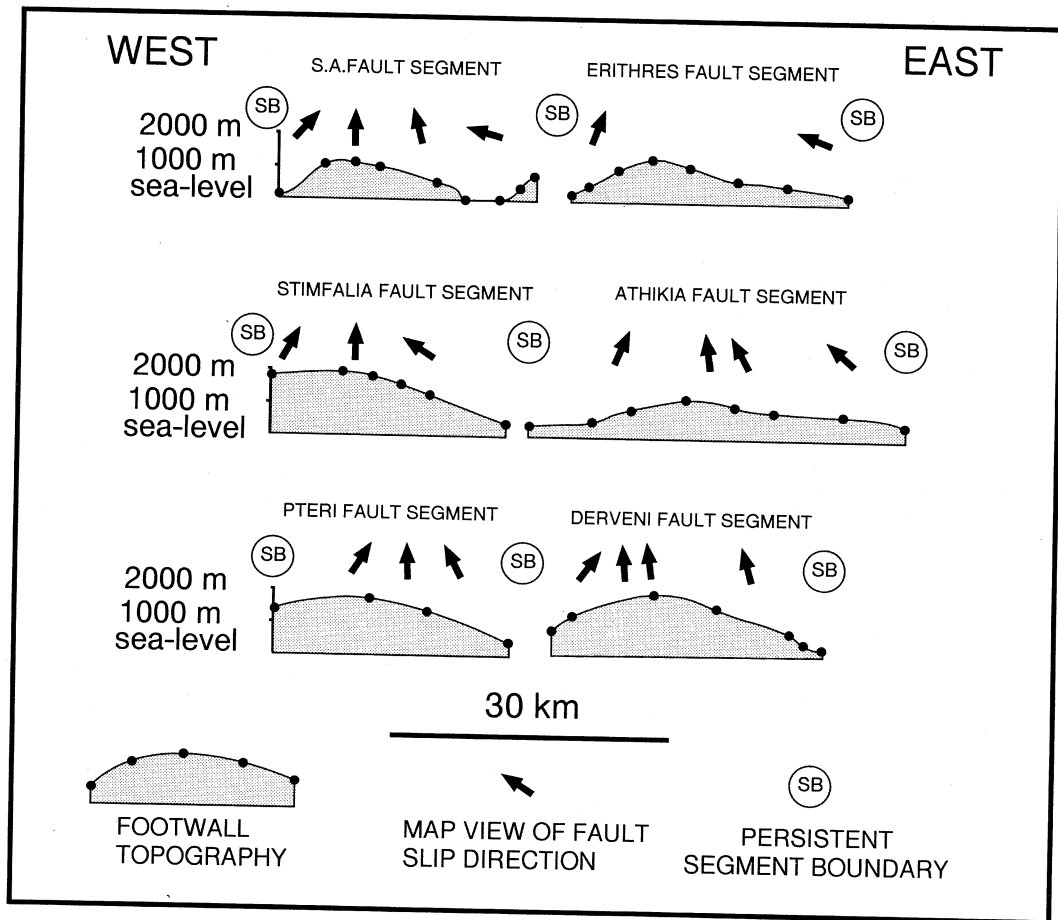
Fig. 7. Topographic profiles along the footwalls of fault segments around the Gulf of Corinth with local fault-slip directions superimposed. The topographic profiles have been constructed using spot heights from published maps (IGME, 1970, 1971, 1982, 1984a,b, 1985, 1989a,b, 1993) to show the highest topography present, without the detail of minor valleys. The increase in footwall topography signifies an increase in fault displacements. Note that maximum footwall topography increases away from persistent segment boundaries characterised by fault-slip directions that are oblique to the regional ~N-S slip vector azimuth. Also note that local fault-slip directions change by ~90° across persistent segment boundaries.

ficult to say conclusively whether it has been ruptured by historical earthquakes; large earthquakes in 1970 (M_s 6.2) and 1928 (M_s 6.3) may have ruptured this fault segment although no submarine or onshore surface faulting has been reported (Ambraseys and Jackson, 1990) (fig. 2b). The fault segment may also have been ruptured in 1981 (Abercrombie *et al.*, 1995) and this is discussed further below.

Displacement gradients along this fault segment can be identified following examination of the spatial variation of the elevation of recent/Quaternary syn-rift reflectors imaged on seismic reflection profiles (Higgs, 1988) (fig. 5b). Isochron maps show that the greatest rates of sediment accumulation and hence subsidence rates exist in the hanging-wall towards the central portion of the fault segment decreasing towards the east and west. Again, the basin which lies offshore of Xilokastron is shaped like a half-spoon, with the bounding faults disappearing into areas of low displacement. Sediment thicknesses thin towards a buried transverse bed-rock ridge in the west and an exposed transverse bed-rock ridge in the east which mark the positions of persistent segment boundaries (fig. 2b).

The fault segment is not exposed on land so that it has not been possible to constrain fault-slip directions using lineations on faults.
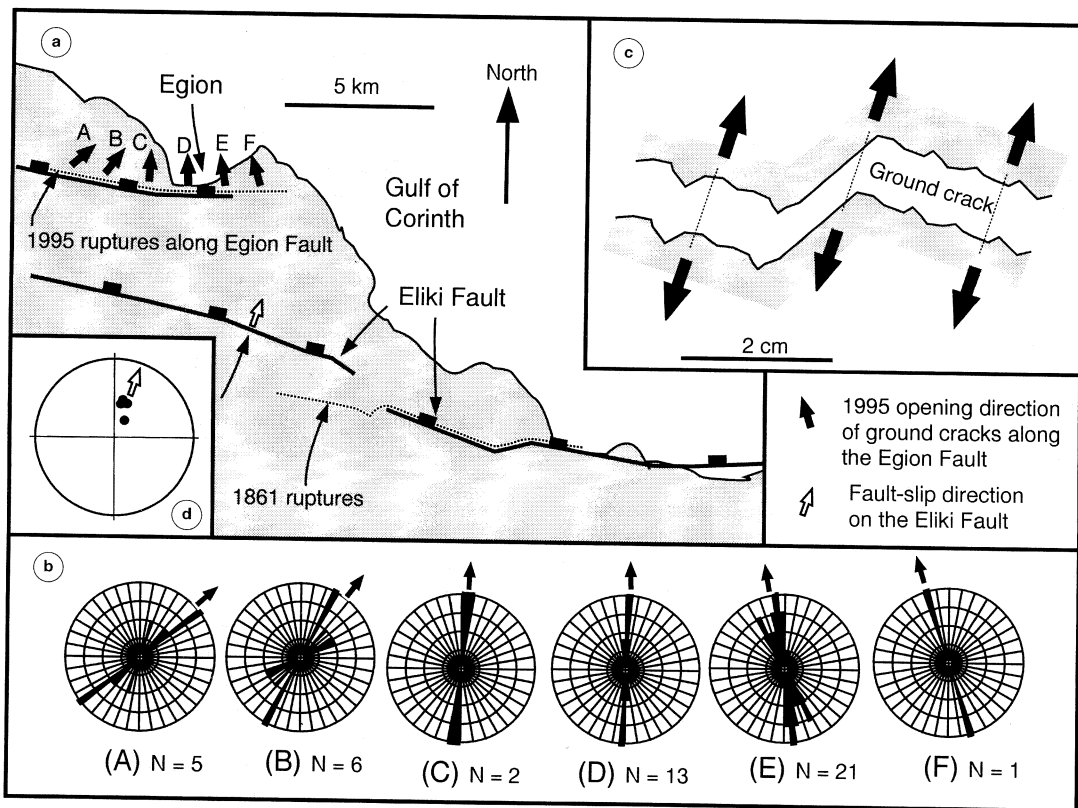
4.4. Egion Fault Segment (EgFS)

A major normal fault system bounds the southern shores of the Gulf of Corinth in this region probably continuing offshore along the line of a bathymetric escarpment (Heezen *et al.*, 1966; Ferentinos *et al.*, 1988; Stewart, 1996). Water depths in the Gulf of Corinth to the north of the fault increase from zero in the west to > 600 m in the east. Large earthquakes (> M 6.0) have occurred in the close proximity to this fault segment in 373 B.C., 1748, 1817, 1861, 1888 and 1995 (Papazachos and Papazachou, 1989; Mouyaris *et al.*, 1992) although only the 1861 and 1995 events are known to have been associated with surface ruptures (Ambraseys and Jackson, 1990; Mouyaris *et al.*, 1992; Stewart, 1996).

The western portion of the segment is most accessible to study, with two major fault-controlled escarpments exposed on land; one along the Eliki Fault lying south of the town of Egion and one along the Egion Fault which runs through the town of Egion (fig. 8a-d). Low fault displacements occur in the west where the crest of the structure plunges west and is blanketed by sheet-like syn-rift deposits of large lateral extent. East from this position, the thicknesses of Quaternary sediments increase eastwards (Poulimenos, 1993) showing that fault-related subsidence also increases in this direction. However, fault displacements must decrease further east; the fault probably continues offshore (Stewart, 1996), forming a marked bathymetric escarpment (Ferentinos *et al.*, 1988), finally dying out where it merges into an area of low fault displacement shown on offshore seismic reflection profiles (Higgs, 1988). Thus, the basin is shaped like a half-spoon, with decreasing fault displacements, subsidence rates and hence fault slip-rates towards the persistent segment boundaries shown in fig. 2b.

Further confirmation that the fault may continue offshore comes from fault-slip data. Fault-slip directions have not been constrained at the western termination of the fault segment which is poorly-exposed or the eastern termination which lies offshore. However, in the centre of the fault segment along the Eliki Fault near Diakofto and Paralia Platanou where displacements are probably greatest, the fault-slip direction is ~N-S (figs. 2a,b and 4). The fact that fault slip directions along the Eliki Fault are oriented ~N-S is an independent line of evidence that the fault continues further west into poorly-exposed ground and east to lie offshore. This is because the terminations of all the other fault segments described in this study are characterised by ~NW-SE or ~NE-SW fault slip directions, suggesting that the Eliki and Egion Faults lie in the central and western portions of the map trace of the EgFS.

4.5. Pteri Fault Segment (PFS)

A major normal fault system bounds the southern side of the Pteri Basin which is filled

Fig. 8a-d a) Map showing part of the Egion Fault Segment and the positions of historical surface ruptures that have occurred in the area. b) Rose diagrams showing the opening directions of ground cracks measured along the surface ruptures to the 1995 Egion earthquake. c) Sketch showing how opening directions were measured from ground cracks. The azimuth of lines joining matching points on the two sides of ground cracks were measured. d) Lower hemisphere stereographic projection showing the fault-slip direction for the Eliki Fault (from Stewart, 1996).

predominantly with coarse-grained fan-delta deposits and is presently perched above sea-level (fig. 2a). There is no evidence that this fault system has been ruptured in historical times by any large normal faulting earthquakes (Ambraseys and Jackson, 1990) (fig. 2b). The Pteri Basin has been uplifted in the footwall of the fault segments that lie to the north, and its sediments are being cannibalised, transported and re-deposited within the Gulf of Corinth.

Displacement gradients along this fault system can be identified following examination of the spatial variation in footwall topography and the dip of the syn-rift to pre-rift contact in the hanging-wall (IGME, 1989a). The footwall topography increases from minima in the east and west of the fault segment (~600 m) to maxima in the centre (~1779 m) (fig. 7) whilst the contact between the pre-rift and syn-rift rocks plunges basinwards in the hanging-wall of the segment (fig. 2a). The bounding faults to this basin disappear at the ends of the fault segment into areas of pre-rift which form transverse bed-rock ridges extending into the hanging-wall (fig. 2b). Spatial variation in fault-slip rates has been postulated for this region following examination of the internal geometry of a stacked system of coarse-grained

fan-deltas exhibiting steep depositional slopes, abrupt thickness changes across faults and limited lateral extent (fig. 5c); the greatest fault slip rates are suggested to lie in the central portions of the proposed fault segment by Gawthorpe *et al.* (1994) and Dart *et al.* (1994), who discuss the interplay between fault-slip rates and climatically-induced base-level changes.

Where fault displacements decrease at the western end of the fault segment near the village of Dafnes, the dominant fault-slip direction is ~NE-SW (figs. 2a,b, 4 and 7). Where fault displacements decrease at the eastern end of the fault segment near the village of Mammousia, the dominant fault-slip direction is ~NW-SE. In the centre of the fault segment where displacements are greatest near the village of Pteri, the dominant fault-slip direction is ~N-S.

4.6. *Derveni Fault Segment (DFS)*

A major normal fault system bounds the southern side of the Derveni Basin which is predominantly filled with coarse-grained fan/delta deposits (figs. 2a,b). This basin, like the Pteri Basin, has been uplifted in the footwall of the fault segments that lie to the north, and its sediments are being cannibalised, transported and re-deposited within the Gulf of Corinth. The basin in the hanging-wall of the DFS is presently perched above sea-level. There is no evidence that this fault system has been ruptured in historical times by any large normal faulting earthquakes (Ambraseys and Jackson, 1990) (fig. 2b).

Displacement gradients along this fault system can be identified following examination of the spatial variation in footwall topography (IGME, 1989b, 1993). The footwall topography is ~600 m where it emerges out of the eastern boundary to the Pteri Fault Segment, increases to ~1757 m in the centre of the Derveni Fault Segment, finally decreasing to sea-level in the east (fig. 7): again the footwall topography resembles a half-dome. Like the Pteri Fault Segment, spatial variation in fault-slip rates can been postulated for this region fol-

lowing examination of the geometry of coarse-grained fan-delta deposits; the greatest fault slip rates are suggested to lie in the central portions of the proposed fault segment (Gawthorpe *et al.*, 1994; Dart *et al.*, 1994).

Where fault displacements decrease at the western end of the fault segment near the village of Pirgos, the dominant fault-slip direction is ~NE-SW (figs. 2a,b, 4 and 7). Where fault displacements decrease at the eastern end of the fault segment near the village of Ano Loutro the dominant fault-slip direction is ~NW-SE. In the centre of the fault segment where displacements are greatest, two localities were examined. Near the villages of Oassi and Aigira the dominant fault-slip direction is ~N-S.

4.7. *Kalavrita Fault Segment (KFS)*

A major normal fault system bounds the southern side of the Kalavrita Basin which is predominantly filled with alluvial and alluvial fan deposits (Doutsos and Poulimenos, 1992; Poulimenos, 1993). This basin, like the Pteri and Derveni Basins, has been uplifted in the footwall of the fault segments that lie to the north and is presently perched above sea-level. There is no evidence to suggest that this fault system has been ruptured in historical times by any large normal faulting earthquakes (Ambraseys and Jackson, 1990).

Displacement gradients along this fault system can be identified following examination of the spatial variation in the dip of the syn-rift to pre-rift contact in the hanging-wall of the fault segment. This contact dips towards the centre of the hanging-wall basin close to the eastern and western segment boundaries with alluvial deposits onlapping onto pre-rift rocks forming transverse bed-rock ridges (figs. 2a,b). Palaeocurrent directions in alluvial fan deposits are to the east at the western end of the basin and to the west at the eastern end of the basin (Poulimenos, 1993) showing that the orientations of syn-depositional slopes support the suggested positions of the fault segment boundaries.

Where fault displacements decrease at the western end of the fault segment near the vil-

lage of Demestiha, the dominant fault-slip direction is ~NE-SW (figs. 2a,b and 4). Where fault displacements decrease at the eastern end of the fault segment near the village of Kalavrita, the dominant fault-slip direction is ~NW-SE. In the centre of the fault segment where displacements are greatest near the village of Vrisari, the dominant fault-slip direction is ~N-S.

4.8. Trikala Fault Segment (TFS)

A major normal fault system bounds the southern side of the Trikala Basin which is predominantly filled with proximal alluvial fan deposits (Doutsos et al., 1988). This basin, like basins described above, has been uplifted in the footwall of the fault segments that lie to the north and is presently perched above sea-level (IGME, 1982, 1993). There is no evidence to suggest that this fault system has been ruptured in historical times by any large normal faulting earthquakes (Ambraseys and Jackson, 1990).

Displacement gradients along this fault system are not well-constrained. The rise in footwall topography from east to west probably defines the eastern segment boundary; the footwall crest is blanketed by syn-rift deposits in the east where low footwall topography exists (fig. 2a). The eastward dip of the pre-rift to syn-rift contact probably defines the western segment boundary (fig. 2a) and this is supported by the observation of Poulimenos (1993) that proximal alluvial fan deposits thin towards this area. The western segment boundary, therefore, appears to be marked by a transverse bed-rock ridge. This fault segment, along with the Kalavrita and Stimfalia Fault Segments, lies within an area with some of the highest topography in the Peloponnese Peninsula. The intense incision by rivers has produced complex geomorphology, and it is this non-fault-related topography which makes the recognition of fault displacements difficult in this region.

At the western end of the fault segment near the village of Agios Varvara, the dominant fault-slip direction, although not constrained by

a large number of data, is probably ~NE-SW, whilst at the eastern end of the fault segment near the village of Trikala, the dominant fault-slip direction is ~NW-SE (figs. 2a,b and 4). In the centre of the fault segment where displacements are probably greatest near the village of Steno, the dominant fault-slip direction is ~N-S.

4.9. Stimfalia Fault Segment (SFS)

A major normal fault system bounds the southern side of the Stimfalia Basin which is predominantly filled with lacustrine, alluvial and colluvial deposits (IGME, 1970, 1982). This basin, like other basins described above, has been uplifted in the footwall of the fault segments that lie to the north and is presently perched above sea-level. There is no evidence to suggest that this fault system has been ruptured in historical times by any large normal faulting earthquakes (Ambraseys and Jackson, 1990).

Displacement gradients along this fault system are revealed by the footwall topography which rises from < 800 m in the east where the crest of the fault is blanketed by syn-rift deposits to over 1900 m in the centre of the fault segment, decreasing further west (fig. 7). High hanging-wall topography exists in the centre of the fault segment separating the hanging-wall basin into two portions, but this is probably a relict pre-extension topographic feature developed during the compressional deformation of the Alpine earth movements. Such thrust belts could contain several kilometres of relief postdating thrusting (e.g., Western Alps); this magnitude of relief would clearly complicate the identification of fault displacements based on topography alone. However, a clear transverse bed-rock ridge exists at the western end of the segment and another buried example may lie at the eastern end (fig. 2b).

At the western end of the fault segment near the village of Likouria, the dominant fault-slip direction is ~NE-SW, whilst at the eastern end of the fault segment near the village of Stimfalia, the dominant fault-slip direction is ~NW-

SE (figs. 2a,b, 4 and 7). In the centre of the fault segment where displacements are probably greatest near the village of Kastanea, the dominant fault-slip direction is ~N-S.

4.10. *Athikia Fault Segment (AFS)*

A major normal fault system bounds the southern side of the Corinth Basin which is predominantly filled with marine marls and conglomerates (IGME, 1970, 1985, 1989a). The Corinth Basin is mainly sub-aerial, but lies very close to sea-level: it is probably being uplifted in the footwall of the SAFS. The AFS may have been ruptured by an earthquake in 1930 (M_s 5.9), but no surface faulting has been reported (Ambraseys and Jackson, 1990) (fig. 2b).

Displacement gradients along this fault system are revealed by the footwall topography (fig. 7) which rises from below sea-level in the east to over 1000 m in the centre of the fault segment, decreasing further west to less than 500 m where the crest of the fault is blanketed by sheet-like syn-rift alluvial deposits of large lateral extent (IGME, 1970, 1985, 1989a).

At the western end of the fault segment near the village of Zyouriai, the dominant fault-slip direction is ~NE-SW (figs. 2a,b, 4 and 7). At the eastern end of the fault segment three localities have been examined, one of which lies on a fault to the north of the main fault; at localities near the villages of Kechries, Katakali and Athikia, the dominant fault-slip direction is ~NW-SE. In the centre of the fault segment where displacements are probably greatest, two localities have been examined; one on the main fault and one on a fault lying further north. The dominant fault-slip directions on faults near the village of Klenia and on the northern side of the hill-top fort of Acro-Corinth are ~N-S.

Future studies may be able to divide these localities between two fault segments. One fault segment may lie to the south and another to the north; the western segment boundary to the possible northern segment may lie buried beneath syn-rift (fig. 2b). However, at present these localities are grouped together as a single fault segment.

4.11. *Summary and discussion*

The descriptions presented above show that displacements across the active normal faults in the studied area are not constant along strike. Displacements vary from tens of metres within areas measuring < 10-15 km along strike which separate fault segments whose displacements achieve maxima of at least ~3 km. There appears to be less displacement accommodated by ~E-W faults in these areas (*e.g.*, Poulimenos *et al.*, 1989), so that the faults segments resemble the isolated fault segments that are envisaged to exist early in the history of an extensional fault system (see Anders and Schlische, 1994). The areas of low fault displacements are interpreted here as areas of the fault system which have been starved of coseismic fault displacement related to ~N-S extension relative to the centres of the segments. Hence using similar reasoning to that used in rifts where a good record of ancient earthquakes exists (Wheeler 1989; Machette *et al.*, 1991; Zhang *et al.*, 1991), the areas of low displacement are interpreted here as persistent segment boundaries, that is, areas where numerous earthquake ruptures have terminated or been interrupted in the past.

Note also that the Gulf of Corinth fault system shows a displacement gradient on a much larger scale: the elevation of hanging-wall basins varies systematically, being 200-400 m above sea-level in the east (Erithres Basin), < 400 m below sea-level in the Alkyonides Basin, > 600 m below sea-level offshore of Xilokastron and then rising from > 600 m below sea-level to a few tens of metres above sea-level along the Egion Fault Segment (figs. 2a,b). This change in elevation of hanging-wall basins over a distance of ~100 km probably characterises a change from distal to medial segments of the Gulf of Corinth fault system, in a similar way to the change in the elevation of range fronts which occurs over comparable distances in other rifts (*e.g.*, the Wasatch Front, Cowie and Scholz, 1992). Rates of uplift in the footwalls of the northern segments implied by the elevations of raised marine deposits also vary along the southern shores of the Gulf of Corinth over a distance of

~100 km being greatest south of the central portion of the Gulf of Corinth: this also probably reflects the change from distal to medial portions of the Gulf of Corinth fault system (compare with Mariolakos and Stiros, 1987).

Returning once again to smaller-scale displacement gradients, it is interesting to note that fault-slip directions vary by ~90° across the proposed persistent segment boundaries (figs. 2a,b and 7): fault-slip directions vary systematically with fault displacements (if footwall topography is used as a guide to fault displacements). This systematic variation of fault-slip directions with fault displacement has not been described to date from other rifts, but an explanation for this phenomena may lie in the suggestion made by Wu and Bruhn (1994) and the observations of Ma and Kusznir (1995) that local shear strains exist at the lateral terminations of fault segments. Ma and Kusznir (1995) show that because footwall uplift is less than hanging-wall subsidence during normal faulting earthquakes (*e.g.*, Stein and Barrientos, 1985), greater along-strike extension occurs in the hanging-wall than in the footwall inducing oblique-slip motions at segment boundaries. On a normal fault dipping to the north, dextral-oblique faulting will occur at the western segment boundary and sinistral-oblique faulting will occur at the eastern segment boundary. The sense of oblique-slip motion recorded in this study agrees well with that proposed by Wu and Bruhn (1994) and Ma and Kusznir (1995), with dextral-oblique faulting close to the western segment boundaries and sinistral-oblique faulting close to the eastern segment boundaries. Thus, it appears that variation in fault-slip directions is a new tool which can be used by field geologists to define the positions of persistent segment boundaries (see Roberts, 1996). The scatter in fault-slip directions recorded for individual localities is also important, and will be discussed in detail later in the paper.

How do the dimensions of fault segments and persistent segment boundaries compare with estimates made by other workers? The persistent segment boundaries proposed herein appear to be of similar dimensions to those proposed in other areas of active normal faulting such as the Western U.S.A. (~10-15 km across) (Zhang *et al.*, 1991). However, because it is not clear exactly where a fault segment finishes and a persistent segment boundary begins, it is not straight-forward to give a value for the length of the fault segments. If the persistent segment boundaries are < 10-15 km across, then some of the fault segments are ~30-35 km long which is similar to the lengths of fault segments reported from the Western U.S.A. (Crone and Haller, 1991; Zhang *et al.*, 1991). However, if the persistent segment boundaries in Central Greece are interpreted to be larger features (~15-25 km across), then the fault segments are shorter, and would be of similar dimensions to those proposed by Roberts and Jackson (1991) (~15-20 km) who interpret segment lengths from geomorphological observations of uplifted areas around the Gulf of Corinth. However, as the relatively-small amounts of fault-related uplift close to persistent segment boundaries could be obscured by uplift related to more regional mechanisms such as underplating within the Hellenic subduction zone (see Collier *et al.*, 1992), the lengths of fault segments could be consistently under-estimated if geomorphological criteria are used in isolation. This may explain why Roberts and Jackson (1991) suggest shorter segment dimensions than the present authors. Also, Roberts and Jackson (1991) do not consider the western continuation of the offshore Xilokastron Fault Segment which is shown on published seismic lines (compare Higgs, 1988 with fig. 1 of Roberts and Jackson, 1991), so that the geometries of the persistent segment boundaries around the Xilokastron and Derveni Fault Segments are shown incorrectly by these authors.

Thus, in summary, the present authors prefer the pattern of fault segments shown in figs. 2a,b to that of Roberts and Jackson (1991) because it is founded on a more complete database and the ratio of fault segment dimensions to segment boundary dimensions is similar to that in other rifts: it appears that some of the fault segments are ~30-35 km long.

5. The geometry and kinematics of historical earthquake ruptures around the Gulf of Corinth

In this section, the geometry and kinematics of the three known surface ruptures for the last ~200 years around the Gulf of Corinth are compared with the geometry and kinematics of the fault segments that hosted the earthquakes: the goal is to constrain how the displacement gradients along the fault segments have developed, and, therefore, which fault behavioural model is most appropriate for probabilistic assessments of earthquake recurrence.

5.1. The 1981 Gulf of Corinth earthquakes

The 1981 Gulf of Corinth earthquakes included two events during the night of 24-25th March (M_s 6.7 and M_s 6.4) and a third M_s 6.2 event on the 4th March (Jackson et al., 1982; Taymaz et al., 1991). The western portion of the South Alkyonides Fault Segment proposed in this study, was ruptured during the night of 24th-25th March (figs. 2b and 6a), producing scarps up to 150 cm high in the centre of the rupture trace, decreasing to zero along strike (fig. 6b). The scarps are located mainly along fault planes developed in Mesozoic bed-rock juxtaposing Mesozoic rocks with recent/Quaternary sediments. Studies of deconvolved broad-band seismological data and 2D finite source models of the deformation suggest that the first event may have ruptured the eastern portion of the offshore Xilokastron Fault Segment (Abercrombie et al., 1995), but we cannot be sure if submarine surface faulting occurred (fig. 2b). The third event ruptured an antithetic fault in the hanging-wall of the Erithres Fault Segment; however, by examining a combination of topography and elevation of the top of the pre-rift Mesozoic rocks it can be shown that the north-dipping portion of the Erithres Fault Segment has a larger displacement (> 600 m) than the south-dipping antithetic fault (~80-100 m) which is probably a second order structure.

The surface ruptures associated with the earthquakes are continuous along-strike for distances of less than ~15 km. Importantly, the surface ruptures associated with the first two earthquakes ruptured only the western end of the South Alkyonides Fault Segment and possibly the eastern end of the offshore Xilokastron Fault Segment proposed herein. Figure 6a-c shows that the onshore rupture terminated, exhibiting its minimum coseismic displacement, in a position coincident with the position of maximum fault displacement along the South Alkyonides Fault Segment. If the offshore Xilokastron Fault Segment was ruptured in the position suggested by Abercrombie et al. (1995), then this rupture also terminated close to the centre of a fault segment in a position where isochron maps show that the greatest hanging-wall subsidence, and presumably, greatest fault displacements exist (fig. 5b).

Coseismic slip vectors measured from along the 1981 scarps (Jackson et al., 1982) (fig. 6a,b) show a swing in orientations that is reminiscent of the pattern of fault slip-directions along the fault segments described earlier in this paper (figs. 2a,b, 4 and 7): both show a pattern converging to the north, but coseismic slip vectors vary over a distance of < 15 km whereas the fault-slip directions vary over a distance of ~30-35 km. Note that there is a large spread in the fault-slip directions recorded at the Skinos-Alepochori locality along the SAFS (fig. 6a-c) with some lineations plunging towards the north-east, that is, around 90° clockwise from the coseismic slip vector recorded in this area following the earthquakes in 1981; this will be discussed further below.

5.2. The 1861 Egion earthquake

The 26th December 1861 Egion earthquake produced surface ruptures along the trace of the Eliki Fault which lies in the central portions of the Egion Fault Segment proposed in this study (Schmidt, 1879; Stewart, 1996) (figs. 2b and 8a-d). The 1861 earthquake has been tentatively proposed as a > M_s 6.0 event based on historical reports of damage. Surface ruptures were described by Schmidt (1879) (see also Mouyaris et al., 1992) and were up to 2.4 m

high in places and 1.8 m wide, achieving a total length of ~13.5 km. No coseismic slip vectors were reported for this earthquake. It appears, therefore, that the 1861 earthquake produced significant surface faulting, but the western and eastern portions of the proposed Egion Fault Segment were left un-ruptured at the surface (fig. 2b).

5.3. *The 1995 Egion earthquake*

The following descriptions of the surface deformation associated with the 1995 Egion earthquakes are only a brief account; a more complete account will be given elsewhere (Koukouvelas and Doutsos, submitted). Firstly, we describe the general form of ground deformation along the Egion Fault, and justify why we think this is the surface expression of co-seismic fault motion at depth. Secondly, we describe some more detailed features of these surface breaks.

The ground surface was deformed by small surface scarps along the EgFS during a sequence of earthquakes that included a M_L 6.2 mainshock and a M_L 5.4 aftershock on June 15th, 1995 (Tselentis *et al.*, 1996) (fig. 8a-d). Initial fieldwork in the first few days after the earthquake (by I. Koukoulevas and T. Doutsos) pin-pointed some surface scarps and instigated a geodetic study that will be reported elsewhere. Despite preliminary press reports, the Eliki Fault appears not to have been ruptured during these earthquakes: instead, surface scarps were located a few tens of metres to the north of a 50-100 high fault-escarpment running through the town of Egion along the clear geomorphic expression of the Egion Fault Escarpment. Observations by I. Koukoulevas and T. Doutsos show that the surface scarps achieved a length of ~7.2 km and had a maximum throw measured at the surface of ~3-5 cm. It was possible to recognise such low values of throw because the scarps occurred within the built-up area surrounding Egion, and where examined displaced tarmac road surfaces, concrete factory floors, tiled patio floors and freshly-cultivated and raked residential gardens. The existence of such features was re-

ported by local people within days of the earthquake and were examined by the authors together with T. Doutsos on 3rd July, 1995 before repair work had begun in earnest.

Note that: 1) the throw on these scarps is small and un-impressive compared to the throw associated with surface ruptures reported for the 1981 and 1861 earthquakes; 2) some of the scarps lie close to the coast where liquefaction features were reported, and 3) it is not easy to reconcile the strike of the scarps with the reported preliminary mainshock focal mechanism (Tselentis *et al.*, 1996). These observations have raised suspicions that these scarps may not be the direct surface expression of coseismic fault motions at depth. Despite this, we believe that several features suggest that these ruptures are the surface expression of coseismic fault motions produced at some point during this sequence of earthquakes:

1) the surface ruptures are fairly straight in map view, cutting inland across coastal deltas: this contrasts with the arcuate pattern of ground deformation associated with liquefaction reported for the 1861 earthquake (Schmidt, 1879), where ground failure phenomena followed the edges of coastal deltas;

2) the ruptures lie along an existing fault which has a clear geomorphic expression;

3) an along-strike gradient in throw along the ruptures is consistent with the pattern expected for fault-related deformation with the greatest throws in the centre of the rupture trace (see below);

4) rupture throws and post-seismic vertical motions mimic the topographic variations along the Egion Fault Escarpment with the greatest values situated where the Egion Fault Escarpment is highest (Koukouvelas and Doutsos, submitted);

5) the pattern of slip-vectors associated with the ruptures are similar to those reported for the 1981 surface breaks which were clearly related to fault motions at depth (see below). We therefore interpret the scarps as surface ruptures produced by coseismic slip along the Egion Fault.

The majority of surface ruptures were ground cracks where all the displacement was parallel to the ground surface, producing open

cracks < 3 cm across. However, ~3-5 cm of vertical motion with downthrow generally to the north occurred on ruptures east of Mantilo Spring and in the floor of a warehouse and car-park sited within a few hundred metres of the entrance to the Egion Ferry Port. The western end of the ruptures (~500 m west of Mantilo Spring) and the eastern end (near Stafidoloma and east of the Church of St. Alexios) were ground cracks: the ground surface was warped vertically by a few centimetres when observed on the 3rd July, 1995, but no vertical motions were noted across the cracks themselves. Thus, the 1995 earthquake rupture appears to have had the greatest vertical displacements towards the centre of its trace and left the central and eastern portions of the Egion Fault Segment un-ruptured.

Careful measurements were made of the direction of opening of the ground cracks by GPR using the methodology shown in fig. 8a-d. The opening-direction could be ascertained with precision because it could clearly be seen how the irregular edges of the cracks fitted together, especially on concrete and tiled floors: a number of measurements were made at each of the individual localities shown in fig. 8a-d. The opening directions show a swing in orientation, defining a movement-azimuth of ~NE-SW at the western end of the ruptures, ~N-S in the centre of the rupture trace and ~NW-SE at its eastern termination. This information may suggest that the coseismic slip vector on the sub-surface fault showed a similar variation in orientation as those associated with the ruptures produced on the 24th-25th February, 1981 on the southern shores of the Gulf of Alkyonides (compare fig. 8a-d with fig. 6a,b).

It is proposed that the Eliki Fault (ruptured in 1861) and the Egion Fault (ruptured in 1995), form part of the Egion Fault Segment described earlier in this paper. If this proposition is accepted, it is noteworthy because this is the only one the fault segments defined in this paper that we know has been ruptured at surface twice in historical times. Note that both the 1861 rupture and the 1995 rupture terminate in almost the same position along the strike of the Egion Fault Segment; the boundary between the two ruptures essentially being a N-S line between the Eliki and Egion Faults. Both ruptures died-out in the central portions of the Egion Fault Segment where the throw is probably greatest: the throw on the 1995 rupture was close to zero at this locality. The NW-SE movement azimuth recorded at the eastern end of the 1995 ruptures contrasts markedly with the N to NE fault-slip direction recorded for the Eliki Fault (fig. 8, and Stewart, 1996).

5.4. *Summary*

All three of the known historical earthquake surface faulting episodes left portions of their host fault segments un-ruptured. Displacements associated with the 24-25th February 1981 ruptures die out where the displacements on the host fault segment (segments?) are probably greatest, as do the displacements on the 1995 ruptures and the surface trace of the 1861 ruptures. Coseismic slip-vector azimuths described for the central portions of the EgFS and SAFS (produced during the 1981 and 1995 earthquakes) are different to the dominant fault-slip directions described earlier in this paper.

It is concluded that the South Alkyonides and Egion Fault Segments cannot have grown through the simple repetition of similar ruptures to those chronicled within the record of historical seismicity: a Characteristic Earthquake Model, where 1) the rupture lengths are the same as the fault segment lengths, and 2) dominant fault-slip directions should be the same as coseismic slip-vector azimuths, cannot explain the growth of the segments described above. Alternative models of fault behaviour should be considered during probabilistic assessments of earthquake occurrence.

6. Discussion of fault behaviour and fault growth

In order to use a probabilistic approach for assessing earthquake occurrence, we must use a model which describes how active faults are

ruptured during successive earthquakes: this is usually the Characteristic Earthquake Model, but as stated above, this may be inappropriate around the Gulf of Corinth. Clearly, palaeo-seismological data are needed for the area, but as mentioned above, information concerning pre-historic earthquakes in Central Greece is still being gathered and is far from complete. It is suggested here that scatter within fault-slip data sets can be used to constrain the behaviour of a single fault segment during a number of earthquake cycles as described below.

Figure 9a-c shows two hypothetical fault segments in (a) map view and (b) on a plot of cumulative fault displacement against length. The fault system has been ruptured by six earthquakes whose ruptures are one half of the length of the fault segments: the fault segments

could be ~30 km long and the ruptures ~15 km long. The number of ruptures is un-important; the main point is that *fault segments* have grown by the temporal variation in the site of the *earthquake segments* with respect to the persistent segment boundaries. Note that the centres of the *fault segments* exhibit larger fault displacements than the persistent segment boundaries, a feature that is common amongst the fault segments described earlier in this paper (compare fig. 7 with fig. 9a-c). The behaviour of the hypothetical fault segments through successive earthquake cycles is closest to the Overlap Model of Schwartz (1989) rather than the Characteristic Earthquake Model, the Uniform Slip Model or the Variable Slip Model described by the same author. However, in contrast to Schwartz (1989),
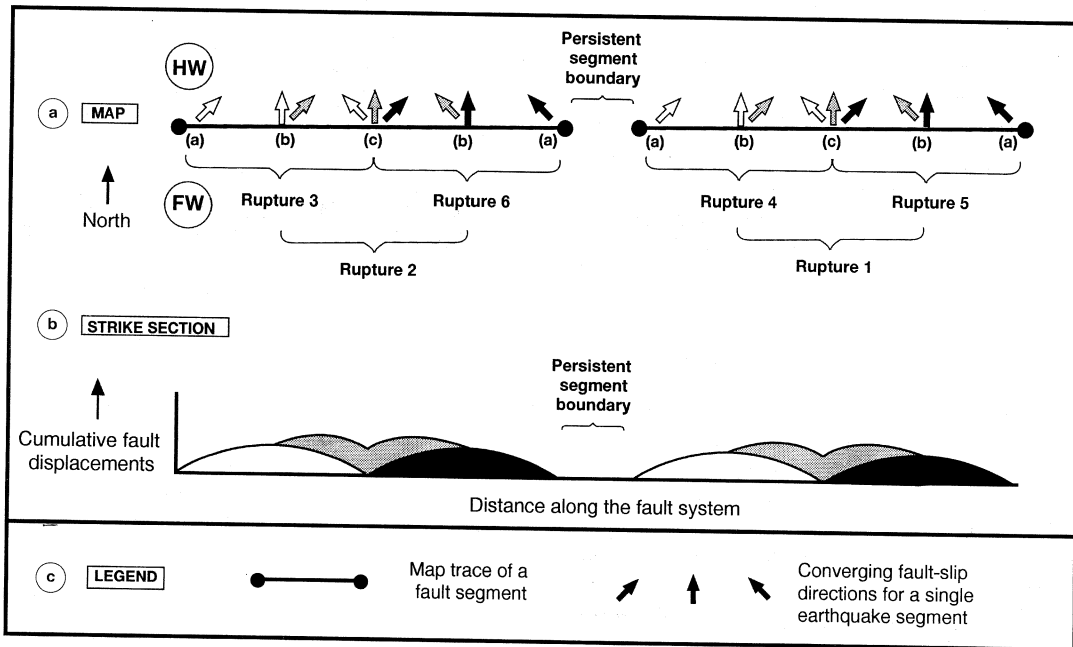
Fig. 9a-c Map views (a) and strike-sections (b) showing the growth of two hypothetical fault segments during six earthquakes, in accordance with a Modified Overlap Model. The pattern of converging coseismic slip vectors towards the hanging-wall for a single rupture has been taken from Jackson *et al.* (1982) and from observations of the 1995 Egion earthquake. At localities labelled (a), the dominant fault-slip directions would be interpreted as 045° or 315° (±0°), at localities labelled (b) as 337.5° and 022.5° (±22.5°) and at locality (c) as 360° (±45°). Note that the greatest scatter in fault-slip directions exists in the central portions of the fault segments.

fig. 9a-c shows a Modified Overlap Model where the overlap zone includes the ends *and* the centres of past earthquake segments rather than solely the ends of earthquake segments (compare figs. 1 and 9a-c). In this model, it may be that ruptures halt both away from and adjacent to fault-zone discontinuities because short-lived lateral variations in stress-level on fault planes augment long-lived structural discontinuities as barriers to rupture propagation.

Let us now consider the scatter in fault-slip directions that would be recorded by lineations on such hypothetical fault segments, and how they would be interpreted by a geologist who has no palaeo-seismological knowledge, that is, the geologist does not know that the lineations were produced by six similar-sized earthquake segments sited at different locations along the fault system. The pattern of converging coseismic slip vectors towards the hanging-wall for a single rupture has been taken from Jackson *et al.* (1982) and the observations of the 1995 Egion earthquakes presented in this study, and plotted for the six ruptures in fig. 9a-c. A geologist would probably interpret the scatter in fault-slip directions at individual localities to represent a single dominant fault-slip direction (as we have done earlier in this paper). At localities labelled (a), the dominant fault-slip directions would be interpreted as 045° or 315° (±0°), at localities labelled (b) as 337.5° and 022.5° (±22.5°) and at locality (c) as 360° (±45°). Note that along the hypothetical fault segments, the persistent segment boundaries have relatively tight clusters of fault-slip directions compared with the centres of the fault segments.

Clearly, the swing in interpreted dominant fault-slip directions displayed by the hypothetical fault system can be used to interpret the positions of persistent segment boundaries as described earlier in this paper (fault-slip directions vary by ~90° across persistent segment boundaries: compare fig. 7 with fig. 9a-c). However, perhaps more importantly, the scatter in fault-slip directions along the hypothetical fault segments may help us to interpret the scatter in fault-slip directions recorded from the fault segments around the Gulf of Corinth: the recorded scatter may contain important in-

formation concerning numerous pre-historic earthquake ruptures. Note that scatter in fault-slip directions produced by characteristic earthquake behaviour would presumably be small and constant along the fault considered, whereas behaviour in accordance with the Modified Overlap Model (fig. 9a-c) produces spatially-variable scatter in fault-slip directions with large values for scatter in the centres of fault segments.

Fault-slip directions on the well-exposed SAFS, where the majority of lineations were measured from the main fault surface shows a similar pattern of scatter in fault-slip directions to the hypothetical fault segments, where the amount of scatter varies spatially (fig. 6c). The greatest scatter is found where fault displacements are greatest on the SAFS (~3 km displacement for the Skinos-Alepochori area), less scatter where fault displacements decrease (700-1000 m displacement in the Pisia-Skinos area) and least scatter where the displacement is smallest (< 200 m for the Psatha locality and perhaps even the Perachora locality). Unfortunately, exposure along the main fault surfaces of most of the other fault segments is poor, so that lineation data was collected from minor faults in the footwall of the main faults and from the main faults themselves. An exception is the KFS where the western and central portions of the main fault surface are well exposed: again the greatest scatter in fault-slip directions is found in the centre of the fault segment with a tighter cluster towards the segment boundary (fig. 4); indeed cross-cutting lineations are clearly visible on the main fault surface in the centre of the segment.

Scatter in fault-slip data for the well-exposed SAFS and KFS may be interpreted as confirmation that the Modified Overlap Model proposed herein may be most appropriate to describe their seismological behaviour when considered over a time-scale long enough to include multiple ruptures of a single fault segment. Indeed, this is precisely the seismological-behaviour exhibited by the Egion Fault Segment during two successive earthquake cycles associated with surface ruptures, that is, the 1861 and 1995 earthquakes. Different portions of the Egion Fault Segment were rup-

tured by these earthquakes and a large scatter in fault-slip directions exists for the centre of the segment if the ~NW-SE coseismic slip vector recorded for the eastern end of 1995 ruptures and the ~N to ~NNE fault-slip direction recorded for the Eliki Fault are combined (fig. 8a-d). However, clearly more work is needed before scatter in fault-slip directions can be used to constrain the seismological behaviour of all the fault segments considered in this study: the fault-slip data for the other fault segments do not appear to fit the simple model described above. One explanation why the data do not fit the model may be that, unfortunately, at the majority of other localities, the fault-slip data were collected from both the main fault planes and smaller fault planes situated within ~10 m of the main fault plane in the footwall due to a lack of good exposure of the main fault surfaces. Presumably some fault-slip directions for footwall faults may contain information pertaining to the localization histories of the fault zones or damage accumulation during slip on the main fault surface (*e.g.*, Roberts, 1994). This may produce greater scatter in fault-slip directions within data sets containing both footwall and main fault surface values, but at present it is not known if this is the case; more work is needed.

The intriguing possibility remains that scatter in fault-slip directions may contain information concerning numerous palaeo-earthquakes on single fault segments; in particular, the positions and dimensions of palaeo-ruptures relative to the host fault segments. This level of palaeo-seismological knowledge has, to date, not been achieved in Central Greece by conventional trenching studies, studies of fault scarp morphology or studies of uplifted coastal notches.

Thus, several lines of evidence appear to confirm that a Modified Overlap Model is more appropriate than the Characteristic Earthquake Model in describing the long term seismological behaviour of *fault segments* around the Gulf of Corinth: 1) scatter in fault-slip directions on the SAFS and KFS; 2) the fact that known historical ruptures did not rupture entire fault segments, and 3) observations of two successive surface ruptures in different positions

along the EgFS. What effect does this have on how we should assess seismic hazards? If the Characteristic Earthquake Model is appropriate, a model where earthquake occurrence is both time- and slip-predictable, it would be feasible to assume a constant earthquake recurrence interval for a particular area and construct maps showing the probabilities of earthquake occurrence within stated time periods; indeed such maps exist for Central Greece (*e.g.*, IGME, 1989a). However, note that if the Modified Overlap Model is appropriate, recurrence intervals will vary both along single fault segments, and with time for single localities (see fig. 9a-c), invalidating the construction of probabilistic maps in the manner described above. We argue above that the Modified Overlap Model is preferable to the Characteristic Earthquake Model and, therefore, suggest that existing probabilistic maps may not prove effective in predicting future earthquake occurrence. Another point is that, using the Characteristic Earthquake Model, we could use the lengths of fault segments as a guide to future earthquake magnitudes. However, unfortunately this would predict ~30-35 km long *earthquake segments* and $> M_s$ 7.0 earthquakes, a pattern that is not borne out by records of historical seismicity (Ambraseys and Jackson, 1990; Mouyaris *et al.*, 1992). In fact over the last ~100 years, *earthquake segments* have been < 15-20 km in length and associated with $< M_s$ ~6.9 events, a pattern which shows some traits of characteristic behaviour (constant maximum magnitudes), but is more consistent with the Modified Overlap Model.

Despite the fact that the Modified Overlap Model predicts future earthquakes which have similar magnitudes and rupture lengths to those documented in historical records, more palaeoseismological data are needed before the possibility of larger earthquakes is forgotten. Unfortunately, studies of scatter in fault-slip directions and cumulative fault displacements would be unable to recognise larger earthquakes $> M_s$ 7.0 interspersed with $< M_s$ 6.9 events, and the return times for such earthquakes could be longer than the reliable portion of the historical record, that is, ~100-200 years. Thus, we do not know whether earth-

quake segments are always shorter than the host fault segments in Central Greece, or, like in the Basin and Range province, earthquakes with long return times (thousands of years) can rupture the entire length of fault segments or multiple fault segments (*e.g.*, de Polo *et al.*, 1991). Thus, conventional studies of the palaeoseismology of the region involving trenching and dating of seismicity at different locations along the same fault segment are needed before the Modified Overlap Model or a model including common $< M_s$ 6.9 events and rare $> M_s$ 7.0 events is confirmed as most appropriate to use in probabilistic modelling of seismic hazards for the region.

7. Conclusions

In areas where palaeo-seismological knowledge derived from conventional studies involving trenching and study of scarp morphologies is limited, alternative methods are needed to constrain the seismological-behaviour of fault segments through a large number of earthquake cycles. Study of: 1) the positions of persistent segment boundaries identified through spatial variation in fault-slip directions, and 2) the scatter in fault-slip directions for individual localities may provide such a method.

It is important to understand the long-term seismological behaviour of fault segments because often studies of seismic hazard use a fault growth model, commonly the Characteristic Earthquake Model, in order to quantify the probabilities of earthquake occurrence and maximum expectable earthquake magnitudes in a region. In the case of the Characteristic Earthquake Model: 1) maximum expected earthquake magnitudes are proportional to the length of the fault segments; 2) the periodicity of earthquakes is slip- and time-predictable, and 3) palaeoseismological observations of earthquake recurrence taken from one locality can be applied to other localities along the same fault segment. However, the evidence presented in this paper suggests that alternative models may be more appropriate to describe the long-term seismological behaviour of the fault segments around the Gulf of Corinth.

Thus, the three attributes of the Characteristic Earthquake Model listed above may not apply to the Gulf of Corinth area, and this should be taken into consideration when attempting to quantify seismic hazards in the region.

REFERENCES

ABERCROMBIE, R. and P. LEARY (1993): Source parameters of small earthquakes at 2.5 km depth, Cajon Pass, Southern California: implications for earthquake scaling, *Geophys. Res. Lett.*, **20**, 1511-1514.

ABERCROMBIE, R., I.G. MAIN, A. DOUGLAS and P.W. BURTON (1995): The nucleation and rupture process of the 1981 Gulf of Corinth earthquakes from deconvolved broad-band data, *Geophys. J. Int.*, **120**, 393-405.

AMBRASEYS, N.N. and J.A. JACKSON (1990): Seismicity and associated strain of Central Greece between 1890 and 1988, *Geophys. J. Int.*, **101**, 663-708.

ANDERS, M.H. and R.W. SCHLISCHE (1994): Overlapping faults, intrabasin highs, and the growth of normal faults, *J. Geol.*, **102**, 165-180.

BILLIRIS, H., D. PARADISSIS, G. VEIS, P. ENGLAND, W. FEATHERSTONE, B. PARSONS, P. CROSS, P. RANDS, M. RAYSON, P. SELLERS, V. ASHKENAZI, M. DAVISON, J. JACKSON and N. AMBRASEYS (1991): Geodetic determination of tectonic deformation in Central Greece from 1900 to 1988, *Nature*, **350**, 124-129.

BONILLA, M.G., R.K. MARK and J.J. LIENKAEMPER (1984): Statistical relations among earthquake magnitude, surface rupture length and surface fault displacement, *Bull. Seism. Soc. Am.*, **74**, 2379-2411.

BROOKS, M. and G. FERENTINOS (1984): Tectonics and sedimentation in the Gulf of Corinth and the Zakynthos

and Kefallinia channels, Western Greece, *Tectonophysics*, **101**, 25-54.

COLLIER, R.E.L1., M.R. LEEDER, P.J. ROWE and T.C. ATKINSON (1992): Rates of tectonic uplift in the Corinth and Megara Basins, Central Greece, *Tectonics*, **11**, 1159-1167.

COWIE, P.A. and C.H. SCHOLZ (1992): Growth of faults by accumulation of seismic slip, *J. Geophys. Res.*, **97**, 11085-11095.

CRONE, A.J. and K.M. HALLER (1991): Segmentation and the coseismic behaviour of Basin and Range Normal Faults: examples from East-central Idaho and South-Western Montana, U.S.A., *J. Struct. Geol.*, **13**, 151-164.

DART, C., R.E.L. COLLIER, R. GAWTHORPE, J.V.A. KELLER and G. NICHOLS (1994): Sequence stratigraphy of (?) Pliocene-Quaternary synrift, Gilbert-type fan deltas, Northern Peloponnesos, Greece, *Mar. Pet. Geol.*, **11**, 545-560.

DE POLO, C.M., D.G. CLARK, D.B. SLEMMONS and A.R. RAMELLI (1991): Historical surface faulting in the Basin and Range province, Western North America: implications for fault segmentation, *J. Struct. Geol.*, **13**, 123-136.

DOUTSOS, T. and G. POULIMENOS (1992): The geometry and kinematics of active faults and their seismotectonic significance in the Western Corinth-Patras Rift (Greece), *J. Struct. Geol.*, **14**, 689-700.

DOUTSOS, T., N. KONTOPOLOUS and G. POULIMENOS (1988): The Corinth-Patras rift as the initial stage of continental fragmentation behind an active island arc (Greece), *Basin Res.*, **1**, 177-190.

FERENTINOS, G., G. PAPATHEODOROU and M.B. COLLINS (1988): Sediment transport processes on an active submarine fault escarpment: Gulf of Corinth: Greece, *Mar. Geol.*, **83**, 43-61.

GAWTHORPE, R.G., A.J. FRASER and R.E.L. COLLIER (1994): Sequence stratigraphy in active extensional basins: implications for the interpretation of ancient basin fills, *Mar. Pet. Geol.*, **11**, 642-658.

HANCOCK, P.L. and A.A. BARKA (1987): Kinematic indicators on active normal faults in Western Turkey, *J. Struct. Geol.*, **9**, 573-584.

HANKS, T.C. and H. KANAMORI (1979): A Moment Magnitude Scale, *J. Geophys. Res.*, **84** (B5), 2348-2350.

HEEZEN, B.C., M. EWING and G.L. JOHNSON (1966): The Gulf of Corinth floor, *Deep-Sea Res.*, **13**, 381-411.

HIGGS, B. (1988): Syn-sedimentary structural controls on basin deformation in the Gulf of Corinth, Greece, *Basin Res.*, **1**, 155-165.

IGME (1970): Nemea 1:50000 Geological Sheet, Athens.

IGME (1971): Erithres 1:50000 Geological Sheet, Athens.

IGME (1982): Kandhila 1:50000 Geological Sheet, Athens.

IGME (1984a): Kaparellion 1:50000 Geological Sheet, Athens.

IGME (1984b): Megara 1:50000 Geological Sheet, Athens.

IGME (1984c): Perachora 1:50000 Geological Sheet, Athens.

IGME (1985): Sofikon 1:50000 Geological Sheet, Athens.

IGME (1989a): Seismotectonic map of Greece 1:500000, Athens.

IGME (1989b): Xilokastron 1:50000 Geological Sheet, Athens.

IGME (1993): Dervenion 1:50000 Geological Sheet, Athens.

JACKSON, J.A. (1994): Active tectonics of the Aegean Region, *Ann. Rev. Earth Planet. Sci.*, **22**, 239-271.

JACKSON, J.A and M.R. LEEDER (1994): Drainage systems and the development of normal faults: an example from Pleasant Valley, Nevada, *J. Struct. Geol.*, **16**, 1041-1061.

JACKSON, J.A. and N.J. WHITE (1989): Normal faulting in the upper continental crust: observations from regions of active extension, *J. Struct. Geol.*, **11**, 15-36.

JACKSON, J.A., J. GAGNEPAIN, G. HOUSEMAN, G.C.P. KING, P. PAPADIMITRIOU, C. SOUFLERIS and J. VIRIEUX (1982): Seismicity, normal faulting, and the geomorphological development of the Gulf of Corinth (Greece): the Corinth earthquakes of February and March 1981, *Earth Planet. Sci. Lett.*, **57**, 377-397.

KELLETAT, D., G. KOWALCZYK, B. SCHRÖDER and K.P. WINTER (1976): A synoptic view on the development of the Peloponnesian coastal regions, *Z. Dtsch. Ges.*, **127**, 447-465.

LE PICHON, X. (1982): Land-locked oceanic basins and continental collision: the Eastern Mediterranean as a case example, in *Mountain Building Processes*, edited by K. HSÜ, 201-211.

LE PICHON, X. and J. ANGELIER (1979): The Hellenic arc and trench system: a key to the neotectonic evolution of the Eastern Mediterranean area, *Tectonophysics*, **60**, 1-42.

MA, X.Q. and N.J. KUSZNIR (1995): Coseismic and post-seismic subsurface displacements and strains for a dip-slip normal fault in a three-layer elastic gravitational medium, *J. Geophys. Res.*, **100** (B7), 12813-12828.

MACHETTE, M.N., S.F. PERSONIUS, A.R. NELSON, D.P. SCHWARTZ and W.R. LUND (1991): The Wasatch Fault zone, Utah - Segmentation and history of Holocene earthquakes, *J. Struct. Geol.*, **13**, 137-150.

MARIOLAKOS, I. and S.C. STIROS (1987): Quaternary deformation of the Isthmus and Gulf of Corinthos (Greece), *Geology*, **15**, 225-228.

MOUYARIS, N., D. PAPANASTASSIOU and C. VITA-FINZI (1992): The Helice Fault? *Terra Nova*, **4**, 124-129.

MYRIANTHIS, M.L. (1982): Geophysical study of the epicentral area of the Alkyonides Islands earthquakes, Central Greece, *Trans. Geophys. Inst. Hungary*, **28** (2), 5-17.

PAPATHEODOROU, G. and G. FERENTINOS (1993): Sedimentation processes and basin-filling depositional architecture in an active asymmetric graben: Strava Graben, Gulf of Corinth, Greece, *Basin Res.*, **5**, 235-253.

PAPAZACHOS, B.C. and K. PAPAZACHOU (1989): *Earthquakes in Greece* (Ziti Publications).

PERISSORATIS, C., D. MITROPOULOS and I. ANGELOPOLOUS (1986): Marine geological research at the Eastern Corinthiakos Gulf, *IGME Geological and Geophysical Research, Athens*, special issue, 381-401.

POULIMENOS, G. (1993): Tectonics and sedimentation in

the Western Corinth Graben, Greece, *N. Jb. Geol. Palaeont. Mh.*, **H10**, 607-630.

POULIMENOS, G., A. GISBERT and T. DOUTSOS (1989): Neotectonic evolution of the central section of the Corinth Graben, *Z. dt. Geol. Ges.*, **140**, 173-182.

ROBERTS, G.P. (1994): Displacement localization and palaeo-seismicity of the Rencurel Thrust Zone, French Sub-Alpine Chains, *J. Struct. Geol.*, **16**, 633-646.

ROBERTS, G.P. (1996): Variation in fault-slip directions along active and segmented normal fault systems, *J. Struct. Geol.*, **18**, 835-845.

ROBERTS, G.P. (1996): Non-characteristic normal faulting surface ruptures from the Gulf of Corinth, Greece, *J. Geophys. Res.* (submitted).

ROBERTS, G.P. and R.L. GAWTHORPE (1995): Strike variation in deformation and diagenesis along segmented normal faults: an example from the Gulf of Corinth, in *Hydrocarbon Habitat in Rift Basins*, edited by J. LAMBIASE, Special Publication of the Geological Society, London, **80**, 57-74.

ROBERTS, S. and J.A. JACKSON (1991): Active normal faulting in Central Greece: an overview, in *The Geometry of Normal Faults*, edited by A.M. ROBERTS, G. YIELDING and B. FREEMAN, Special Publication of the Geological Society, London, **56**, 125-142.

SCHMIDT, J. (1879): *Studien uber Erdbeben*, Leipzig, 68-83.

SCHOLZ, C.H. (1989): Comments on models of earthquake recurrence, in *Proceedings of Conference XLV «Fault Segmentation and Controls of Rupture Initiation and Termination»*, edited by D.P. SCHWARTZ and R.H. SIBSON, *U.S. Geol. Surv. Open-file Rep.*, 89-315, 350-360.

SCHWARTZ, D.P. (1989): Paleoseismicity, persistence of segments, and temporal clustering of large earthquakes - examples from the San Andreas, Wasatch, and Lost River fault zones, in *Proceedings of Conference XLV «Fault Segmentation and Controls of Rupture Initiation and Termination»*, edited by D.P. SCHWARTZ and R.H. SIBSON, *U.S. Geol. Surv. Open-file Rep.*, 89-315, 361-375.

STEIN, R.S. and S.E. BARRIENTOS (1985): Planar high-angle faulting in the Basin and Range: Geodetic analysis of the 1983 Borah Peak, Idaho, earthquake, *J. Geophys. Res.*, **90**, 11355-11366.

STEWART, I. (1996): Holocene uplift and paleaoseismicity on the Eliki Fault, Western Gulf of Corinth, Greece, *Annali di Geofisica*, **39**, 575-588 (this volume).

TAYMAZ, T., J.A. JACKSON and D.P. MCKENZIE (1991): Active tectonics of the north and central Aegean, *Geophys. J. Int.*, **106**, 433-490.

TSELENTIS, G-A., N.S. MELIS, E. SOKOS and K. PAPATSIMPA (1996): The Egion June 15, 1995 (6.2 M_L) earthquake, *PAGEOPH* (in press).

VITA-FINZI, C. and G.C.P. KING (1985): The seismicity, geomorphology and structural evolution of the Corinth area of Greece, *Philos. Trans. R. Soc. London*, Ser. A, **314**, 379-407.

WHEELER, R.L. (1989): Persistent segment boundaries on Basin-Range normal faults, in *Proceedings of Conference XLV «Fault Segmentation and Controls of Rupture Initiation and Termination»*, edited by D.P. SCHWARTZ and R.H. SIBSON, *U.S. Geol. Surv. Open-file Rep.*, 89-315, 432-444.

WU, D. and R.L. BRUHN (1994): Geometry and kinematics of active normal faults, South Quirrh Mountains, Utah: implication for fault growth, *J. Struct. Geol.*, **16**, 1061-1076.

WYSS, M. (1979): Estimating maximum expectable magnitude of earthquakes from fault dimensions, *Geology*, **7**, 336-340.

ZHANG, P., D.B. SLEMMONS and F. MAO (1991): Geometric pattern, rupture termination and fault segmentation of the Dixie Valley-Pleasant Valley active normal fault system, Nevada, U.S.A., *J. Struc. Geol.*, **13**, 165-176.